INITIAL EVALUATION OF SEASONAL YIELD AND IRRIGATION DEMAND FORECASTING FRAMEWORKS FOR OKLAHOMA

By

BRANDON ALBIN VAVERKA

Bachelor of Science in Agronomy

Oklahoma Panhandle State University

Goodwell, OK

2016

Submitted to the Faculty of the
Graduate College of the
Oklahoma State University
in partial fulfillment of
the requirements for
the Degree of
MASTER OF SCIENCE
December, 2018

INITIAL EVALUATION OF SEASONAL YIELD AND

IRRIGATION DEMAND FORECASTING

FRAMEWORKS FOR OKLAHOMA

Thesis Approved:

Dr. Phillip Alderman

Thesis Adviser

Dr. Tyson Ochsner

Dr. Jason Warren

ACKNOWLEDGEMENTS

I would like to thank my advisor Dr. Phillip Alderman for his assistance in guiding me through my graduate career. Also, I would like to include my committee members Dr. Tyson Ochsner and Jason Warren. Last but not least, I would like to thank my parents Chris and Lynda Vaverka.

Name: BRANDON ALBIN VAVERKA

Date of Degree: DECEMBER, 2018

Title of Study: INITIAL EVALUATION OF SEASONAL YIELD AND IRRIGATION DEMAND FORECASTING FRAMEWORKS FOR OKLAHOMA

Major Field: PLANT AND SOIL SCIENCES

Abstract: Climate variability plays a large role in agriculture. Having the proper tools to investigate the effects of climate variability in agriculture is necessary to better understand our future. Wheat, corn, and cotton are three crops important in Oklahoma. These crops can all be effected by climate variability. One method of understanding the problem is through crop modeling frameworks. The objective of this thesis is to investigate the utility of modeling frameworks in Oklahoma. The studied was carried out by using the Decision Support System for Agrotechnology Transfer – Cropping System Model (DSSAT-CSM) framework. The crops focused on are wheat, corn, and cotton. The weather data, soil data, and model configurations were tested to find out how they performed. Chapter 2 covers a wheat yield forecasting study, and chapter 3 covers irrigation demand forecasting. Overall, the models supply an understanding of how modeling frameworks are relative to Oklahoma, and can be used. The limitations to the models are input data, initial conditions, and management practices. There is still a lot of room for improvement in the models discussed in this thesis such as calibrating cultivars to the study area, but it does provide a basis for future research.

TABLE OF CONTENTS

LIST OF TABLES

TABLES IN CHAPTER II

TABLES IN CHAPTER III

LIST OF FIGURES

FIGURES IN CHAPTER I

FIGURES IN CHAPTER II

Figure Page

FIGURES IN CHAPTER III

Figure Page

CHAPTER I

GENERAL INTRODUCTION

Water scarcity has played a significant role throughout the history of Oklahoma. Dry years are often followed by wet years as illustrated by Figure 1. Multiple definitions of drought exist, but drought is typically defined as a period during which precipitation is insufficient to meet the established needs of a region (Arndt 2002). Rainfall has a direct impact on agriculture causing drought to have large economic impact. The 2002 drought in Oklahoma witnessed a $150 million crop loss in winter wheat (Arndt 2002). The estimated agricultural losses for the 2011 drought in Oklahoma was $2 billion (Tadesse et al. 2015). Agriculture accounts for close to 70% of the water withdrawn from surface water and ground water around the world (Wisser et al. 2008). Producers use irrigation to supplement rainfall to reduce the impact of limited water availability. For best results, water is applied at critical stages of plant development. The supplement of rainfall with irrigation becomes more complicated during a drought because the recharge of the ground water is not keeping up with the water needs of the crop. This raises the possibility of unsustainable irrigation water use. Agricultural irrigation water demand is driven by numerous factors such as acreage and type of crop irrigated, irrigation system, water availability, and fuel and commodity prices (OWRB 2011). Climate variability further contributes to the uncertainty in irrigation demand (Döll 2002).

Oklahoma is in the Great Plans region where a high variability for crop yields exist (Ray et al. 2015). Variability in rainfall, and temperature can have a dramatic impact on crop yields (Wang et al., 2003; Hatfield and Walthall, 2015; Zampieri et al., 2017). Crop models can be used to help determine the impact of climate variability (Rosenzweig et al., 1994; Lobell et al., 2008). Crop models can be employed to assess the risk involved in management decisions. This could lead to a more effective way to manage inputs more efficiently to save money and resources. Crop models also have the ability to help understand future risk through probabilistic forecasting. A probabilistic forecast produces a range of possible values instead of a single value as in a deterministic model. Probabilistic yield forecasting can be a viable option for producers to see what their range of anticipated yields are for a specific season, and utilize the best management practices for the season given that yield range. This ability could lead to more effective use of inputs, contributing to cost savings for the producer.

This thesis is organized into two studies. Chapter II addresses wheat yield forecasting, and focuses on the development and evaluation of a wheat yield forecasting framework for Oklahoma. Chapter III addresses irrigation demand, and evaluates initial simulation conditions and data inputs for spatially quantifying irrigation demand for corn and cotton in Oklahoma. Chapter IV summarizes the finding of Chapter II and II, and then ties those findings back to the main objective.

Objective

- Evaluate the relevance of simulation modeling frameworks in Oklahoma

REFERENCES

Arndt, D. S. (2002), *The Oklahoma drought of 2001-2002*, Oklahoma Climatological Survey.

Döll, P. (2002), Impact of climate change and variability on irrigation requirements: A global perspective, *Climatic Change*, *54*(3), 269–293.

Hatfield, J. L., and C. L. Walthall (2015), Meeting global food needs: Realizing the potential via genetics X environment X management interactions, *Agronomy Journal*, *107*(4), 1215–1226.

Lobell, D. B., M. B. Burke, C. Tebaldi, M. D. Mastrandrea, W. P. Falcon, and R. L. Naylor (2008), Prioritizing climate change adaptation needs for food security in 2030, *Science*, *319*(5863), 607–610.

OWRB (2011), Oklahoma comprehensive water plan 2012 update: Water demand forecast report,

Ray, D. K., J. S. Gerber, G. K. MacDonald, and P. C. West (2015), Climate variation explains a third of global crop yield variability, *Nature Communications*, *6*, 5989.

Rosenzweig, C., M. L. Parry, and others (1994), Potential impact of climate change on world food supply, *Nature*, *367*(6459), 133–138.

Tadesse, T., B. D. Wardlow, J. F. Brown, M. D. Svoboda, M. J. Hayes, B. Fuchs, and D. Gutzmer (2015), Assessing the vegetation condition impacts of the 2011 drought across the us southern great plains using the vegetation drought response index (vegdri), *Journal of Applied Meteorology and Climatology*, *54*(1), 153–169.

Wang, W., B. Vinocur, and A. Altman (2003), Plant responses to drought, salinity and extreme temperatures: Towards genetic engineering for stress tolerance, *Planta*, *218*(1), 1–14.

Wisser, D., S. Frolking, E. M. Douglas, B. M. Fekete, C. J. Vörösmarty, and A. H. Schumann

(2008), Global irrigation water demand: Variability and uncertainties arising from agricultural and climate data sets, *Geophysical Research Letters*, *35*(24).

Zampieri, M., A. Ceglar, F. Dentener, and A. Toreti (2017), Wheat yield loss attributable to heat waves, drought and water excess at the global, national and subnational scales, *Environmental Research Letters*, *12*(6), 064008.

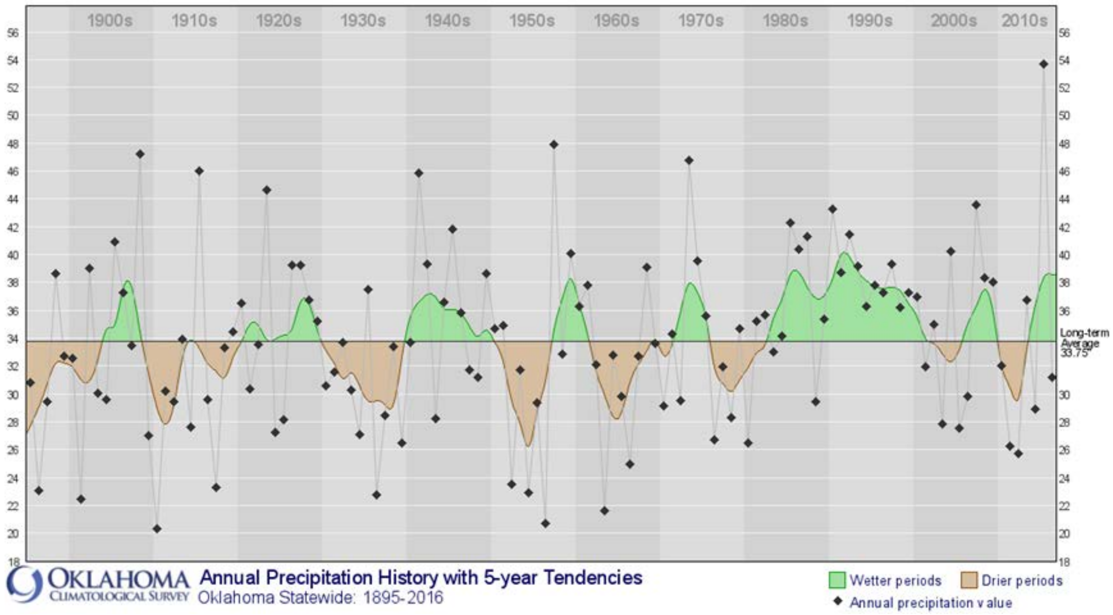

Figure 1: Precipitation history of Oklahoma

CHAPTER II

DEVELOPMENT AND EVALUATION OF A PROBABILISTIC WHEAT YIELD FORECASTING FRAMEWORK FOR OKLAHOMA

Abstract

Oklahoma is in the Great Plans region where a high variability for wheat yields exists (Ray et al., 2015). Variability in rainfall, and temperature can have a dramatic impact on wheat yields (Wang et al., 2003 Zampieri et al. (2017); Hatfield and Walthall, 2015). This creates a need for analyzing the future uncertainty involved with wheat yields. Crop modeling frameworks can aid in the forecasting of wheat yield. Using DSSAT-CSM and CERES Wheat, a probabilistic wheat yield modeling framework was produced. The objectives of this study were to develop a wheat yield forecasting framework for Oklahoma, find the earliest weeks after planting a prediction can be made, and analyze the effect of initial conditions on the model. It was able to predict yield percentile as early as 5 to 15 weeks after planting with a threshold window of 33% and 28 to 32 weeks after planting for a threshold window of 10%. Overall, there is still a need for further study to perfect the modeling framework.

1. Introduction:

Oklahoma is in the Great Plans region where a high variability for wheat yields exist (Ray et al., 2015). Wheat is a common crop in Oklahoma. In 2017 4.5 million acres were planted, 98.6 million bushels were harvested, and it resulted in a production value of $379.6 million (NASS, 2017). Variability in rainfall and temperature can have a dramatic impact on wheat yields (Wang et al., 2003; Hatfield and Walthall, 2015; Zampieri et al., 2017). This creates a need for analyzing the future uncertainty involved with wheat yields. Crop modeling frameworks can aid in the forecasting of wheat yield.

Yield forecasting can be a viable option for producers to see which management options may perform the best under current season conditions. This ability could lead to more effective use of fertilizers, contributing to cost savings for the producer. For example, a producer could be making a decision concerning top-dressing nitrogen on his wheat crop. With yield forecasting, the producer would be able to see a probabilistic estimate in advance to help make his or her decision. Also yield forecasting could be beneficial to marketing agencies to prepare for grain handling, and whether they should hold onto their current grain or sell it.

Many methods have been evaluated to find the most reliable way to predict yield with varying success. Moriondo et al. (2007) attempted to create a simple wheat yield model based on satellite NDVI data in the Mediterranean climate of Italy, and discovered using remotely sensed data to drive crop models helped make up for lack of input data required by extensive crop models. They also found spatial resolution of the satellite NDVI data played a big role in the accuracy of predicted yield. Shamseddin and Adeeb (2012) focused on producing accurate, simple and low-cost crop yield prediction models. They found that correlation between crop yield and NDVI were low in their area of Sudan.

Studies have been done to assess affect of drought on crop yield. Walker (1989) created a model to replicate wheat yields in Western Canada for 10 years, and found the model was able to explain 92% of the variance in the average wheat yield by using only monthly precipitation and temperature variables as input. In some cases, weather has to be estimated to make up for lack in input data for weather variables. Bannayan et al. (2003) tried to determine if the CERES-Wheat model could be used to forecast final grain yield and crop biomass within the growing season. They used the SIMMETEO weather generation algorithm in DSSAT to generate the daily weather data from averaging four weather stations in the UK. They found grain yield simulations were accurate, and that updating the model within the growing season with measured data helped the accuracy of the model. Yield prediction models have been found to provide similar results in different locations. Becker-Reshef et al. (2010) developed an empirical regression model in Kansas to be used in Ukraine, and found the model performed well with 8 years of data from Ukraine. Greene and Maxwell (2007) used 35 years of historical climatological data and the CERES-Wheat model to forecast current season wheat yield at various weather stations across Oklahoma. They found the station based model to be a good predictor of actual yields, and the model was able to reproduce the variability of past season recorded wheat yields in Oklahoma. So far, little has been studied pertaining to the effects of using multiple spatial data sets, and finding the effects of model configurations for the same region.

When creating gridded outputs, it is good to note the optimum spatial resolution. Easterling et al. (1998) studied the optimum spatial resolution of observed climate and soils data for simulating maize and wheat in the Central Great Plains. They found that close to a 1 degree (111 km) spatial resolution provided effective results when mapping a region the size of the Great Plains. Similarly, (De Wit et al. 2005) analyzed the spatial resolution of yield simulation data in Germany and France, and found sub-grid variability exists, but the 10 x 10 km grid had no advantage to the 50 x 50 km grid for accurately predicting total wheat yield over a region.

Crop yield forecasts have been carried out to determine the accuracy of predicted yield, and how far in advance of harvest a prediction can be made. Li et al. (2016) assessed the yield forecast performance of the CERES-Wheat model in China with increasing nitrogen inputs. They found yield fluctuation of predicted yield was similar with different nitrogen input conditions, and noted as the proportion of observed weather data increased during the season the predicted yields became more accurate. Nain et al. (2004) tested the accuracy of CERES-Wheat model to see year-to-year variability in a large area of wheat located in Central Indo-Gangetic Plains of India. They found forecasting 6 weeks prior to harvest is possible without sacrificing accuracy.

Crop models do have limitations. Chipanshi et al. (1997) set up a simulation for forecasting wheat yield in Saskatchewan. The simulation used current in-season data up to the prediction date, and used historical data to estimate the rest of the season. They stated that CERES-Wheat provided advantages to empirical models, but noticed a lack of sensitivity to disease and pest damage in the CERES-Wheat model compared to observed data. Kogan et al. (2013) found winter wheat forecasting in Ukraine worked best in areas with greater homogeneity in landscape vegetation cover. Lee et al. (2013) performed a study estimating county wheat yield and wheat quality by using weather information. They noted that extreme weather conditions, such as a late season freeze, could not be recognized by their empirical model and in return, negatively affected the yield forecast accuracy. Also crop models can vary in results by the weather data used as inputs. O'Neal et al. (2002) completed a study that determined the viability of on-farm precipitation measurements. They used three precipitation data sources and found the effect of spatial variability of precipitation on yield was 15.8%, and the effect of temporal variability was 20.5%.

In summary simulation models are an effective way of predicting end-of-season yield. They have limitations due to lack of dense input data and insensitivity to certain factors such as, spatial resolution of the satellite imagery, weather phenomena, pests, and diseases, but have been shown to give a good representation of anticipated yield at harvest. The goal of this research is to support the development of a probabilistic yield modeling frame work.

Objectives

The objectives of this study were to:

- Develop a wheat yield forecasting framework for Oklahoma
- Find the earliest yield prediction point after planting
- Analyze the effect of initial condition on the model simulations

2. Materials and Methods:

2.1 Crop Models:

The Decision Support System for Agrotechnology Transfer Cropping Systems Model (DSSAT-CSM; Jones et al., 2003) is a crop modeling system with multiple modules. CROPSIM-CERES Wheat (Thorp et al., 2010) models are computer simulated models for wheat which incorporate crop management decisions such as planting date, fertilizer rate, and irrigation scheduling to simulate crop growth and development. Climate, soil, and cultivar selection are the main inputs to run the model. Driving the wheat forecasting tool is the CROPSIM-CERES Wheat (Thorp et al., 2010) model. The cultivar used was Newton. Newton is already parameterized in the CERES-Wheat model. The planting date was set at October 15th, and was simulated as grain only production. Initial soil moisture was set at 50% of available water capacity. The simulation start date was set at July 1. For the automatic planting option, DSSAT selects a planting date using soil temperature and moisture. A planting window has to be given using the parameters PFRST and PLAST. PFRST is the first day the simulation can begin planting, and PLAST is the last day the simulation can plant. Simulation start date was set to July 1 to allow the soil moisture to "spin-up" in the model prior to the planting date. The R package called dssatR (Alderman, 2014) has been written to facilitate linking DSSAT to R. The dssatR package contains functions to build experiment files, soil files, and incorporate weather files using an R interface. The DSSAT-CSM is a point-based model. Thus, an interface was written to allow the model to read and write data in Network Common Data Format (NetCDF), a widely-used gridded data format. The interface was designed to be flexible to allow for gridded simulations at any resolution.

2.2 Weather and Soil Data:

Weather data was derived from Inverse Distance Weighted (IDW) Mesonet data. The Oklahoma Mesonet (McPherson et al., 2007) is a network of 121 automated environmental monitoring stations. There is at least one station per county in Oklahoma. Each station has a 10-meter tall tower, and environment observations are made every 5 minutes. For this study, daily summary data from the Mesonet were interpolated through Inverse Distance Weighting (IDW) using the R package gstat (Gräler et al., 2016). For this study, data interpolated using a power value of 1 to create a nominally 5 km grid. Soil type for each 5 km grid box was selected as the soil type with the largest areal coverage within the grid box. Variables used for simulation included daily maximum and minimum air temperature, cumulative daily solar radiation, 2 meter average wind speed. Soil data were derived from STATSGO2 which is the Digital General Soil Map of the United States which estimates soil types based on landscape and is displayed at a scale of 1:250,000 (Soil Survey Staff, 2017). Soil lower limit (SLLL), drained upper limit (SDUL), and saturated soil moisture (SSAT) were set to STATSGO2 values of soil moisture at -1500, -30, and 0 kpa, respectively. Missing values for these variable were estimated using nearest neighbor analysis based on soil texture and saturated conductivity. Runoff curve number was estimated using hydrologic soil group (HSG) and slope. Missing HSG values were estimated using soil depth and saturated conductivity based on (NRCS, 2004). Values for soil drainage rate (SLDR) parameter were estimated using the drainage class from STATSGO2 and the get.sldr function from dssatR (Alderman, 2014) For missing drainage class values SLDR was assumed to be 0.6. Values for Soil nitrogen mineralization factor (FLNI) and soil productivity factor (SLPF) were both set to 1.0.

2.3 Yield forecast Framework:

Base simulations were created for each growing season from 1997 to 2016 using the actual observed weather for each season. The yields were simulated for the prior 19 years using weather data and soil data as described in section 2.1, 2.2., and simulation condition represented by (**) in reference Table 1. A wheat yield forecasting framework was developed that can combine in-season measurements of precipitation with estimates of future precipitation derived from past and current weather data. The framework simulates each possible future to provide a probabilistic estimate of current season yield. Forecast dates were set at two-week intervals from 2 to 32 weeks through the growing season to determine how soon after planting an accurate prediction could be made for yield. The yields were displayed spatially on a 5 km grid across Oklahoma. Simulated yields were converted to percentiles to allow the yields to be categorized relative to historical yields as below average, average, and above average. The yields were converted into percentiles by creating Wheat yields were assumed to be normally distributed across seasons, and the pnorm function in R was used to express the yield as a percentile. The mean and standard deviation were calculated from the baseline simulated yields for each pixel of the grid.

The model generates a probabilistic forecast based off past seasons. As illustrated in Figure 1, weather data for the current season were used until a given forecast date. Weather data for driving simulations for the remainder of the season were taken from other seasons. For example, for the 2-weeks-after-planting forecast date of the 2015-16 season, the 2015-16 season data were used until two weeks after planting. Subsequently, one forecast scenario used weather data from 1997-1998 for the rest of the season. Another forecast scenario followed the same procedure except using weather data from 1998-1999. This process was repeated for all seasons of available weather data resulting in an ensemble of 19 forecasted yields for the 2015-2016 season. This ensemble was used to generate the forecast range for 2015-2016 at two weeks after planting. This same process was repeated on a biweekly interval from 4 to 32 weeks after planting. A prediction was made when a week in the season reached a specified threshold. The threshold was based on the size of the interquartile range (IQR) of the percentile yield. So when 50% of the simulations were within a given range is when the model would make a prediction. The sizes of the IQR used in the study were 10 and 33 percentile difference between Q1 and Q3. The 33rd percentile was chosen because it could be categorized as low yielding, average yielding, and high yielding. The 10th percentile was chosen so we could see where the prediction date was when using a narrow IQR window.

2.4 Model Configuration Testing:

In order to evaluate the effect of different model configurations on simulated yield, baseline simulations were run for each year, 1997-2015 with varying model configuration to test effects of initial soil moisture and planting date. Planting date was set to automatic planting. For the simulations, PFRST was set at September 1st, and then a second simulation was run with PFRST set at October 1st. PLAST was set to December 31st for both simulations. All model configuration testing simulation are outlined in Table 1.

3. Results:

The forecasted yield is expressed here as percentiles based on the mean and standard deviation of baseline simulations for each grid point. The prediction date is expressed as weeks after planting because of variability in harvest date. Figure 2 shows box-plots of possible yield at each forecast date (Weeks After Planting) for the 1997-1998 season at a point near Medford, OK. Typically, the range in possible yield percentile was large for the forecasts made at start of the season. As the forecast date became later, the range in possible yield reduced. In Figure 2 the model would have made the prediction for the 33% threshold at 22 weeks and 32 weeks for the

10% threshold. Figure 3 shows the distribution of possible yield at each forecast date. In Figure 3, the interquartile range is smaller at the beginning of the season and grows larger as the season progresses, and does not shrink down until 28 weeks after planting. The weather has a large impact in increasing or decreasing these yield windows. In this case the model would have made a prediction at 28 weeks for the 33% threshold and 32 weeks for the 10% threshold. In Figure 4 the interquartile range is large at the beginning and gets smaller in the middle as the season progresses, but becomes larger again towards the end of the season. However the last box plot at 32 weeks after planting is small with a <10% interquartile range. So both the 33% and 10% thresholds would have made a prediction at 32 weeks after planting.

Figures 5 and 6 show the difference between maximum and minimum forecasted percentile yield at selected weeks after planting for the 2010-2011 season. The yield percentile does not start to converge until 24 weeks after planting. The forecast percentile for most of the state at week 32 shows little difference between maximum and minimum forecasted yield. However, even at 32 weeks after planting there are some areas in North Central and the Panhandle that still show a difference.

Figure 7 and 8 shows the average prediction time across Oklahoma with an interquartile threshold set at 33% and 10% respectively. On average, yield percentile could be predicted between 5-15 weeks after planting with a 33% threshold (Fig 7). Areas of southwest Oklahoma had a higher prediction time of >18 weeks after planting. Forecasts for the majority of the wheat growing area converged within 5-15 weeks after planting. For the 10% threshold the average prediction time after planting was between 27 and 32 weeks (Fig 8). North Central and far southwest saw the lowest prediction time while most of Central and Southwest saw a later prediction time. Figure 9 shows the standard deviation in the prediction time with the threshold set at 33% across all 19 simulation years. Most of the state had a standard deviation between 3 to 9 weeks. North Central and most of Southwest Oklahoma had a standard deviation of 4 to 7 weeks after planting. Parts of Central Oklahoma had a standard deviation less than 3 weeks. However, areas in the Panhandle and along the Cimmaron, and Canadian rivers had a standard deviation higher than 8.

Figure 10 shows the standard deviation in the prediction time with the threshold set at 10%. The standard deviation using 10% threshold was lower than using the 33% threshold. The standard deviation in prediction times with the 10% threshold varied between 3 to 6 weeks. Some parts of Central Oklahoma and the Panhandle had a standard deviation of less than 3 weeks.

Simulation with varying model configurations were compared to the base simulations by taking the difference between the average of the configuration scenario and the average of the baseline simulation.

Setting the initial soil moisture to 100 percent plant available had a positive impact on yield. Most areas saw a 0 to 25 percentile increase (Fig. 11). Changing the initial soil moisture to 0 percent plant available water had a negative impact on yield. The yield percentile decreased by 10 to 30 for most parts of the state (Fig. 12). Setting the model to automatically plant between October 1 and December 31 increased the yield percentile between 5 and 25 (Fig. 13). The typical Oct. 1 simulated planting dates had a minimum day of year date of 274, maximum of 300, and average of 283. The September 1 simulated planting dates had a minimum day of year date of 244, 300 maximum date, and average date of 250. Pixels where yield percentile is missing shows that conditions for planting were not met during the planting window. Parts of western Oklahoma and the Panhandle had the largest gains in yield of above 20 percentile. Setting the model to automatically plant between September 1 and December 31 increased yield percentile between 0 and 20 for most of the state (Fig. 14). Central Oklahoma and parts of the Panhandle had the highest increase in yield percentile.

4. Discussion:

4.1 Within-season yield variability:

The model was able to create the variability in the range of forecasted yields throughout the growing season, and show how the range gets closer to the final yield. At the beginning of the season there was a wide range of possible yields. As the season progressed the range of yield possibilities diminished leaving a narrow window at the end of the season. This trend would be expected because at the beginning of the season there is more opportunity to produce higher yields than there is at the end of the season close to harvest where little can be done to change the outcome of yield. This decreasing window of yield potential was also noted by (Chipanshi et al., 2015). Some years and locations experience an abrupt narrowing and broadening in the range of the yield window. The yield range would shrink to a certain point then become larger again. The driving factor behind the size of these windows changing is the weather. Intense rainfall or lack of rainfall can cause a swing in the yield ranges. In general, the range of yield at the prediction time is small enough to place into categories of low yielding, average yielding, and high yielding. This can be beneficial, because just knowing what kind of year it's going to be can have an impact on management decision producers are going to make. In low yielding years, less inputs such as fertilizer, fungicide, and pesticide would be used to save money from having low yields.

4.2 Earliest weeks after planting:

Using the basic assumptions of same planting date, variety, dry-land, same management practices, the average weeks after planting for most of the state where it was possible to forecast the rest of the season was between 28 to 32 weeks after planting for the 10% threshold, and 5 to 15 weeks for the 33% threshold. If wheat was planted on October 15 and harvested the first week in June, that would make the growing season close to 33 weeks long. So the model with the 10% threshold would make a prediction 1 to 4 weeks before harvest and the 33% threshold 17 to 27 weeks before harvest. That would be similar to Mkhabela et al. (2011) where they were able to make a prediction 1 to 2 months prior to harvest. It may not be enough time to make management decisions such as graze-out or top dressing N, but it could prepare the producer for financial planning. It would still be enough time for marketing agencies to prepare for wheat harvest. Adjusting the threshold had an effect on the standard deviation on the annual variability of the prediction time. The reason is the 10% threshold typically predicted later in the season. A prediction later in the season has less chance of a large increase or decrease in yield because the season is pretty much determined at that point. A lot of the issues in the model may be caused by the basic assumptions of same management practices, variety selection, and planting date. The uncertainty in the model could be from input data, the basic assumptions, and the model itself. Walker et al. (2003) described these uncertainties for model-based decision support activities.

4.3 Changing model configuration:

Changing the model configuration provided information about running simulations in the future. Some configurations had more influence than others. The base simulation soil moisture was set at 50%, and compared to two other base simulations at 100% and 0% initial soil moisture. The 100% initial soil moisture simulation was dramatically higher than the 0% initial soil moisture. There was close to a 40 percentile difference between two simulations. The different initial soil moisture values possibly effected the soil moisture at the time of planting. This could be caused by the amount of rainfall in between the simulation start date and time of planting. Using measured soil data could have made the simulations more accurate. Setting up the model for automatic planting provided interesting results. Changing the planting window from 1 September-31 December to 1 October- 31 December did not make much difference. However, large areas in the 1 October- 31 December simulation did not plant. It is possible soil temperature and moisture thresholds for planting should be relaxed for better estimation of initial condition should be provided.

5. Conclusion:

The model was able to give a probabilistic forecast of wheat yield in Oklahoma, and demonstrate the in-season variability of yield ranges across the season. The model was able to make a prediction as early as 5 to 15 weeks after planting at a 33% threshold, and 28 to 32 weeks after planting with a 10% threshold. The range of yield percentile is small enough to categorize into below average yielding, average yielding, and above average yielding. Initial conditions do play a role in model performance. Wheat yield forecasting can be a viable option for Oklahoma to aid in mitigating the effect of climate variability. However, there is still a lot of research to be done to make it effective.

REFERENCES

Alderman, P. D. (2014), *DSSATR: R interface to DSSAT-CSM models*.

Bannayan, M., N. Crout, and G. Hoogenboom (2003), Application of the CERES-Wheat model for within-season prediction of winter wheat yield in the United Kingdom, *Agronomy Journal*, *95*(1), 114–125.

Becker-Reshef, I., E. Vermote, M. Lindeman, and C. Justice (2010), A generalized regression-based model for forecasting winter wheat yields in Kansas and Ukraine using MODIS data, *Remote Sensing of Environment*, *114*(6), 1312–1323.

Brock, F. V., K. C. Crawford, R. L. Elliott, G. W. Cuperus, S. J. Stadler, H. L. Johnson, and M. D. Eilts (1995), The Oklahoma Mesonet: A technical overview, *Journal of Atmospheric and Oceanic Technology*, *12*(1), 5–19.

Chipanshi, A., E. Ripley, and R. Lawford (1997), Early prediction of spring wheat yields in Saskatchewan from current and historical weather data using the CERES-Wheat model, *Agricultural and Forest Meteorology*, *84*(3), 223–232.

Chipanshi, A., Y. Zhang, L. Kouadio, N. Newlands, A. Davidson, H. Hill, R. Warren, B. Qian, B. Daneshfar, F. Bedard, and others (2015), Evaluation of the Integrated Canadian Crop Yield Forecaster (ICCYF) model for in-season prediction of crop yield across the Canadian agricultural landscape, *Agricultural and Forest Meteorology*, *206*, 137–150.

De Wit, A. d, H. Boogaard, and C. Van Diepen (2005), Spatial resolution of precipitation and radiation: The effect on regional crop yield forecasts, *Agricultural and Forest Meteorology*, *135*(1), 156–168.

Easterling, W. E., A. Weiss, C. J. Hays, and L. O. Mearns (1998), Spatial scales of climate information for simulating wheat and maize productivity: The case of the US Great Plains, *Agricultural and Forest Meteorology*, *90*(1), 51–63.

Gräler, B., E. Pebesma, and G. Heuvelink (2016), Spatio-temporal interpolation using gstat, *The R Journal*, *8*(1), 204–218.

Greene, J. S., and E. Maxwell (2007), Climatic impacts on winter wheat in Oklahoma and potential applications to climatic and crop yield prediction, *International Journal of Biometeorology*, *52*(2), 117–126.

Hatfield, J. L., and C. L. Walthall (2015), Meeting global food needs: Realizing the potential via genetics X environment X management interactions, *Agronomy Journal*, *107*(4), 1215– 1226.

Jones, J. W., G. Hoogenboom, C. H. Porter, K. J. Boote, W. D. Batchelor, L. Hunt, P. W. Wilkens, U. Singh, A. J. Gijsman, and J. T. Ritchie (2003), The DSSAT cropping system model, *European Journal of Agronomy*, *18*(3), 235–265.

Kogan, F., N. Kussul, T. Adamenko, S. Skakun, O. Kravchenko, O. Kryvobok, A. Shelestov, A. Kolotii, O. Kussul, and A. Lavrenyuk (2013), Winter wheat yield forecasting in Ukraine based on earth observation, meteorological data and biophysical models, *International Journal of Applied Earth Observation and Geoinformation*, *23*, 192–203.

Lee, B.-H., P. Kenkel, and B. W. Brorsen (2013), Pre-harvest forecasting of county wheat yield and wheat quality using weather information, *Agricultural and Forest Meteorology*, *168*, 26–35.

Li, Z., M. Song, H. Feng, and Y. Zhao (2016), Within-season yield prediction with different nitrogen inputs under rain-fed condition using CERES-Wheat model in the northwest of China, *Journal of the Science of Food and Agriculture*, *96*(8), 2906–2916.

Liu, H., J. Yang, C. al Drury, W. Reynolds, C. Tan, Y. Bai, P. He, J. Jin, and G. Hoogenboom (2011), Using the DSSAT-CERES-Maize model to simulate crop yield and nitrogen cycling in fields under long-term continuous maize production, *Nutrient Cycling in Agroecosystems*, *89*(3), 313–328.

McPherson, R. A., C. A. Fiebrich, K. C. Crawford, J. R. Kilby, D. L. Grimsley, J. E. Martinez, J. B. Basara, B. G. Illston, D. A. Morris, K. A. Kloesel, and others (2007), Statewide monitoring of the mesoscale environment: A technical update on the Oklahoma Mesonet, *Journal of Atmospheric and Oceanic Technology*, *24*(3), 301–321.

Mkhabela, M., P. Bullock, S. Raj, S. Wang, and Y. Yang (2011), Crop yield forecasting on the Canadian prairies using MODIS NDVI data, *Agricultural and Forest Meteorology*, *151*(3), 385–393.

Moriondo, M., F. Maselli, and M. Bindi (2007), A simple model of regional wheat yield based on NDVI data, *European Journal of Agronomy*, *26*(3), 266–274.

Nain, A., V. Dadhwal, and T. Singh (2004), Use of CERES-Wheat model for wheat yield forecast in central Indo-Gangetic Plains of India, *The Journal of Agricultural Science*, *142*(1), 59–70.

NASS (2017), USDA/NASS 2017 state agriculture overview for Oklahoma,

NRCS (2004), National engineering handbook: Part 630—Hydrology, *USDA Soil Conservation Service: Washington, DC, USA.*

O'Neal, M. R., J. R. Frankenberger, and D. R. Ess (2002), Use of CERES-Maize to study effect of spatial precipitation variability on yield, *Agricultural Systems*, *73*(2), 205–225.

Ray, D. K., J. S. Gerber, G. K. MacDonald, and P. C. West (2015), Climate variation explains a third of global crop yield variability, *Nature Communications*, *6*, 5989.

Shamseddin, A. M., and A. M. Adeeb (2012), Using remotely sensed and ancillary data to predict spatial variability of rainfed crop yield, *International Journal of Remote Sensing*, *33*(12), 3798–3815.

Soil Survey Staff (2017), *Web soil survey*, Natural Resources Conservation Service, United States Department of Agriculture.

Thorp, K. R., D. J. Hunsaker, A. N. French, J. W. White, T. R. Clarke, and P. J. Pinter Jr (2010), Evaluation of the CSM-CROPSIM-CERES-Wheat model as a tool for crop water management, *Transactions of the ASABE*, *53*(1), 87–102.

Walker, G. (1989), Model for operational forecasting of western canada wheat yield, *Agricultural and Forest Meteorology*, *44*(3-4), 339–351.

Walker, W. E., P. Harremoës, J. Rotmans, J. P. van der Sluijs, M. B. van Asselt, P. Janssen, and M. P. Krayer von Krauss (2003), Defining uncertainty: A conceptual basis for uncertainty management in model-based decision support, *Integrated Assessment*, *4*(1), 5–17.

Wang, W., B. Vinocur, and A. Altman (2003), Plant responses to drought, salinity and extreme temperatures: Towards genetic engineering for stress tolerance, *Planta*, *218*(1), 1–14.

Zampieri, M., A. Ceglar, F. Dentener, and A. Toreti (2017), Wheat yield loss attributable to heat waves, drought and water excess at the global, national and subnational scales, *Environmental Research Letters*, *12*(6), 064008.

Table 1: Model configurations.

Initial Soil Moisture	**Planting type**	**Planting Date**
0% PAWC	Fixed	15 Oct
100% PAWC	Fixed	15 Oct
**50% PAWC	**Fixed	**15 Oct
50% PAWC	Fixed	15 Oct
50% PAWC	Automatic	1 Sep – 31 Dec
50% PAWC	Automatic	1 Oct – 31 Dec

(**) Indicates configuration used for baseline simulation

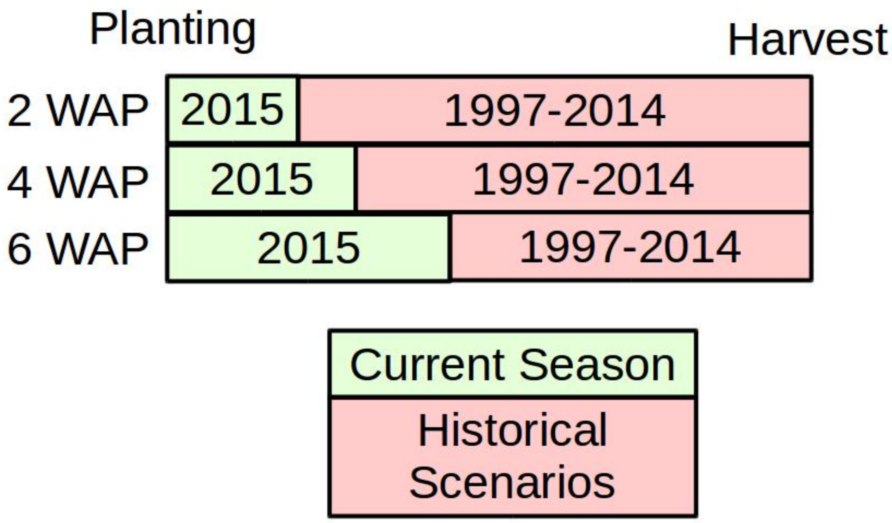

Figure 1: Model schematic

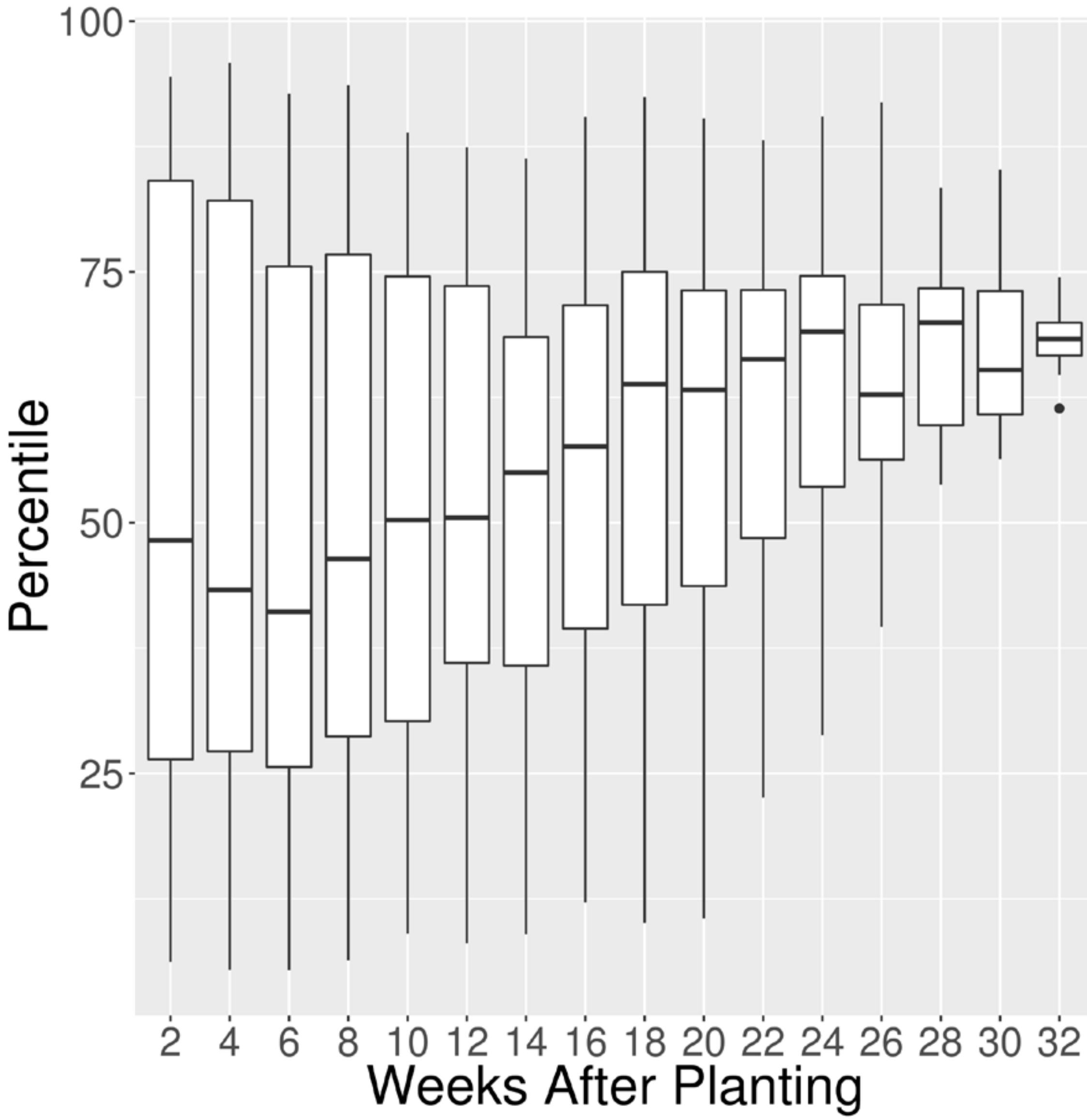

Figure 2: Change in distribution of forecasted yield percentile for a location near Medford, OK for the 1997-1998 season. Yield percentile of forecasted yields were calculated based on the mean and standard deviation of simulated yields for the same location from the 1997 to 2016 seasons. The whiskers show the maximum and minimum yield percentile. The box ends are Q2 on top, and Q3. Q2 represents 25% of the simulations and Q3 is 75% of the simulations. The line in the middle is 50% of the simulations.

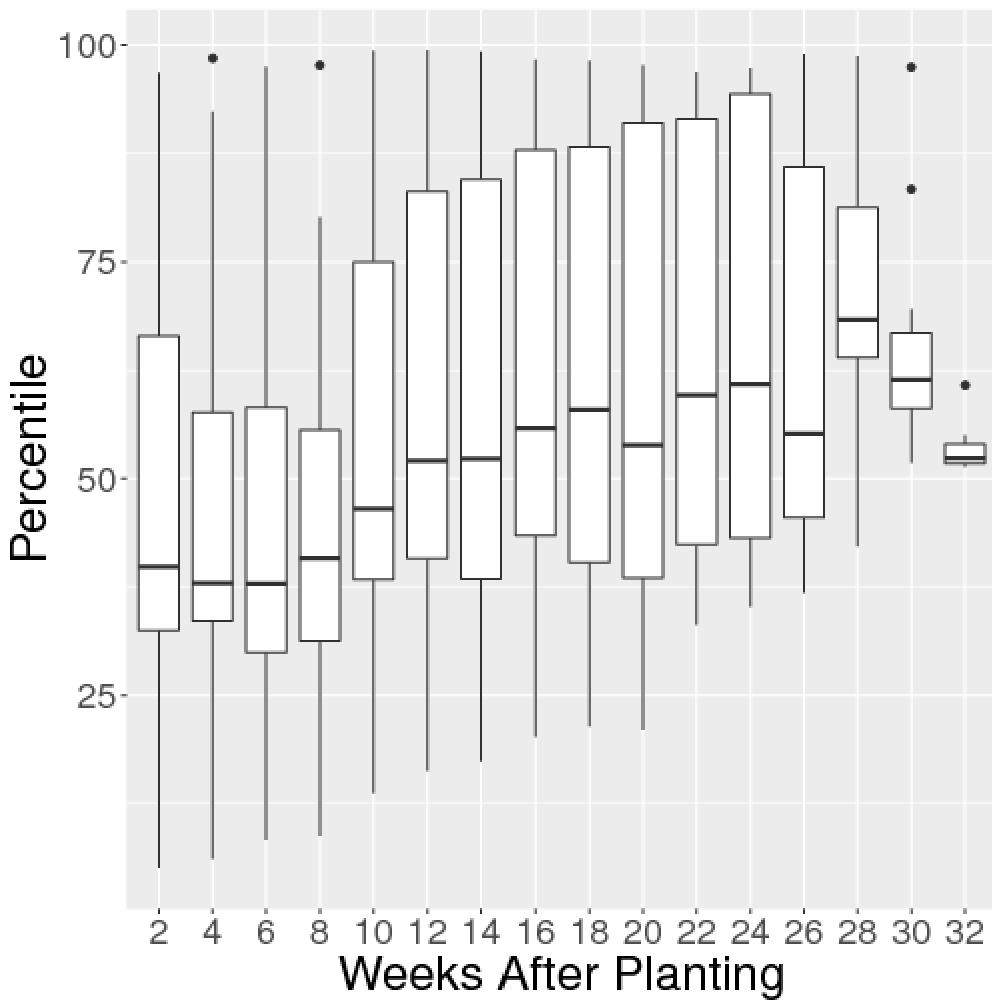

Figure 3: Change in distribution of forecasted yield percentile for a location near Chickasha, OK for the 1997-1998 season. Yield percentile of forecasted yields were calculated based on the mean and standard deviation of simulated yields for the same location from the 1997 to 2016 seasons. The whiskers show the maximum and minimum yield percentile. The box ends are Q2 on top, and Q3. Q2 represents 25% of the simulations and Q3 is 75% of the simulations. The line in the middle is 50% of the simulations.

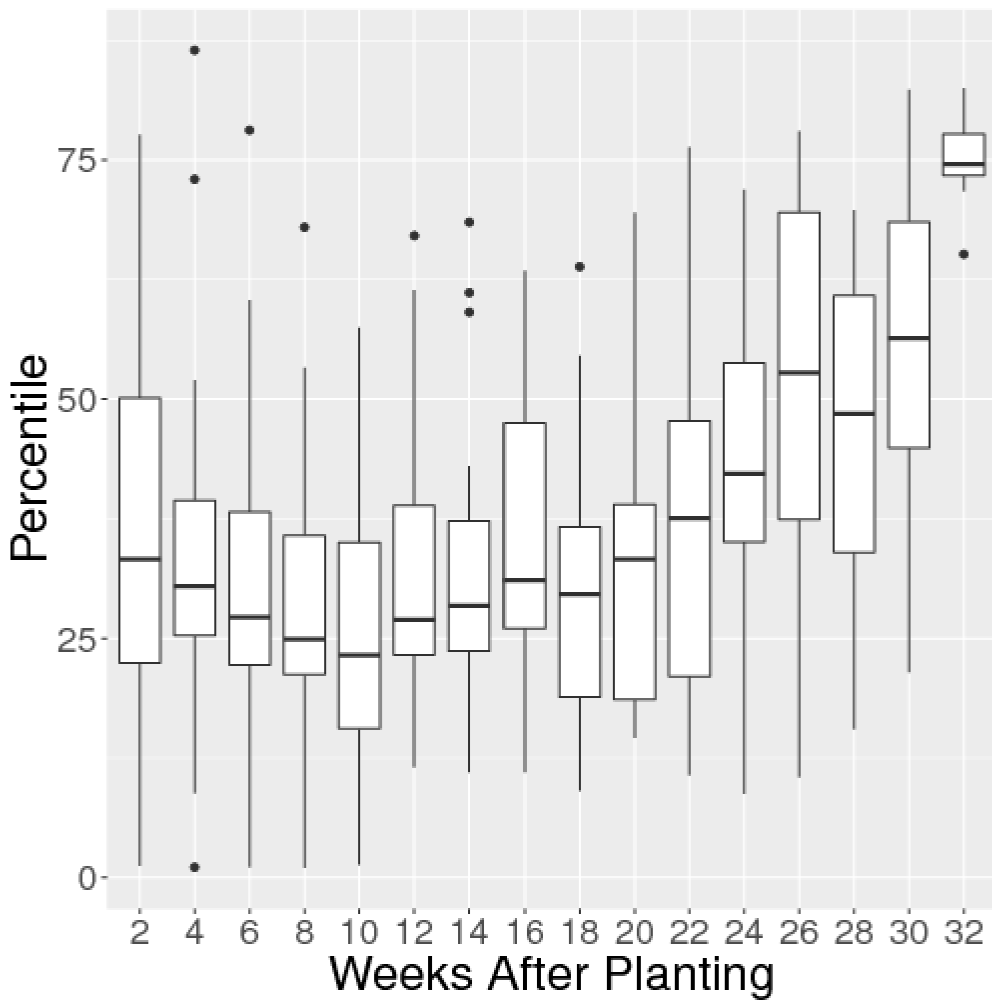

Figure 4: Beaver, OK 2000-2001 season Change in distribution of forecasted yield percentile for a location near Beaver, OK for the 2000-2001 season. Yield percentile of forecasted yields were calculated based on the mean and standard deviation of simulated yields for the same location from the 1997 to 2016 seasons. The whiskers show the maximum and minimum yield percentile. The box ends are Q2 on top, and Q3. Q2 represents 25% of the simulations and Q3 is 75% of the simulations. The line in the middle is 50% of the simulations.

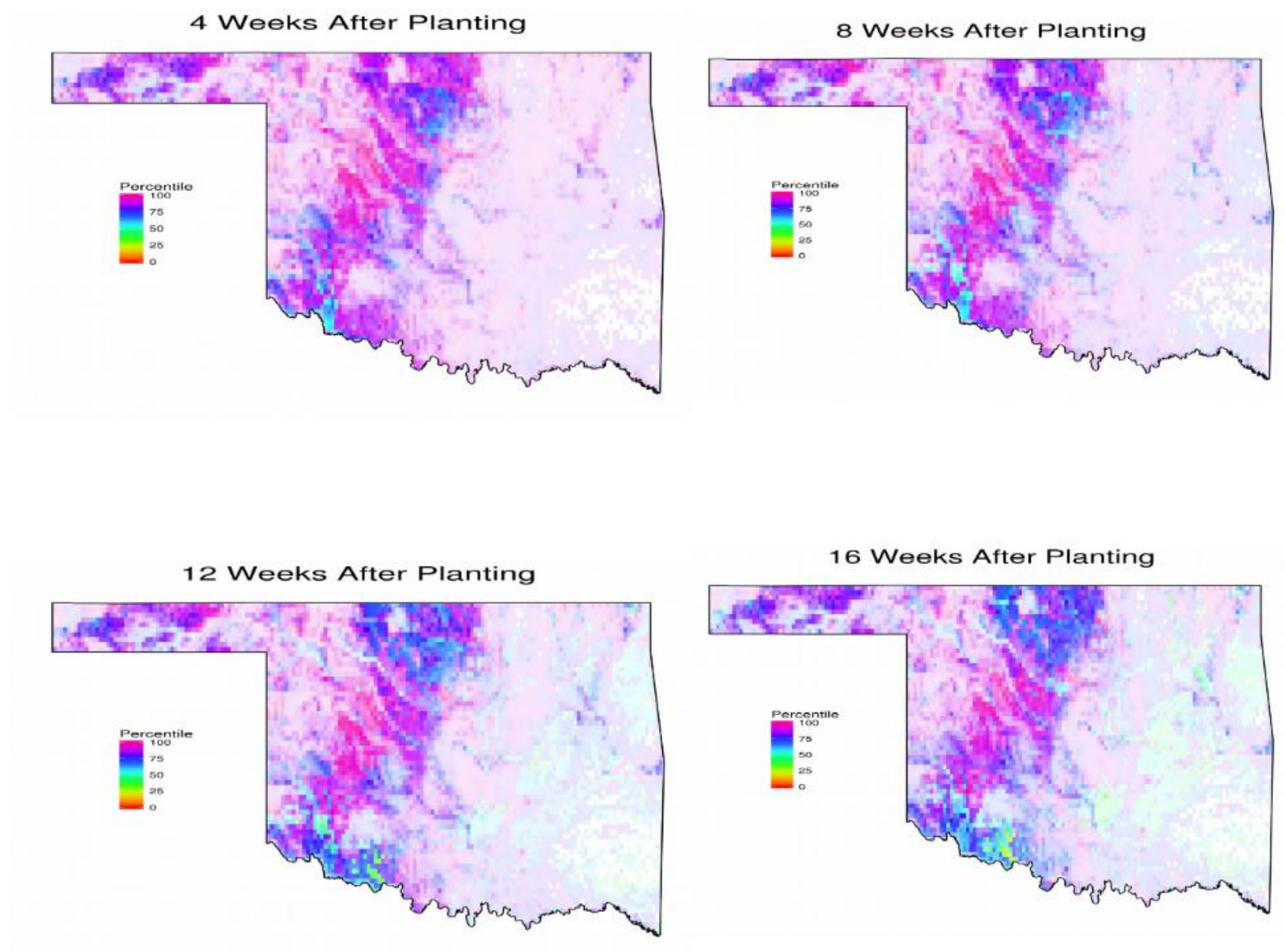

Figure 5: Spatial distribution of the difference between the highest and lowest forecasted yield percentile at different forecast dates for Oklahoma in the 2010-2011 season. Forecasted yield percentiles were calculated based on the mean and standard deviation of simulated yields from the 1997 to 2016 seasons. Opacity of pixel indicates fraction of pixel in wheat land use for at least one season between 2008 to 2016 as determined by the Cropland Data Layer.

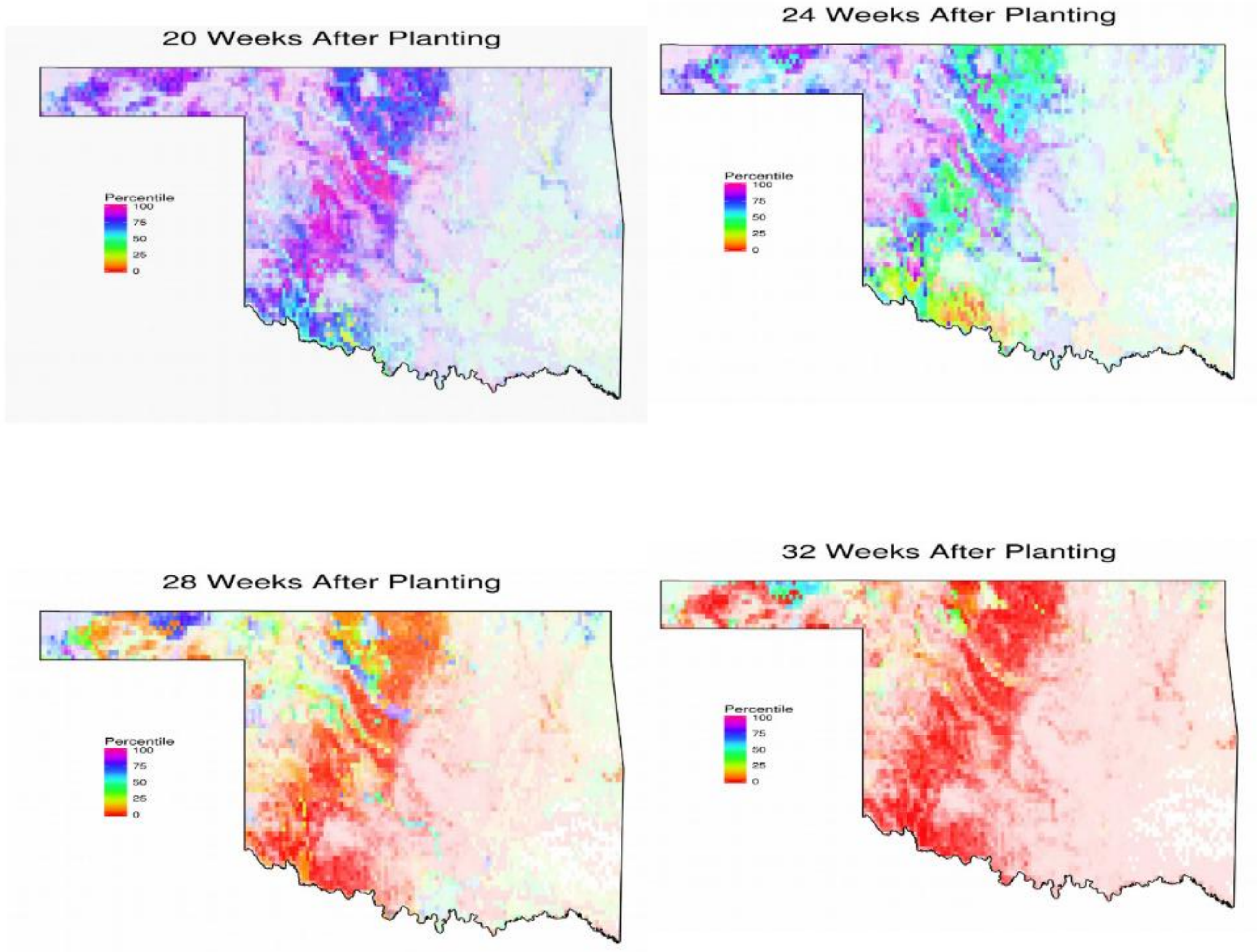

Figure 6: Spatial distribution of the difference between the highest and lowest forecasted yield percentile at different forecast dates for Oklahoma in the 2010-2011 season. Forecasted yield percentiles were calculated based on the mean and standard deviation of simulated yields from the 1997 to 2016 seasons. Opacity of pixel indicates fraction of pixel in wheat land use for at least one season between 2008 to 2016 as determined by the Cropland Data Layer.

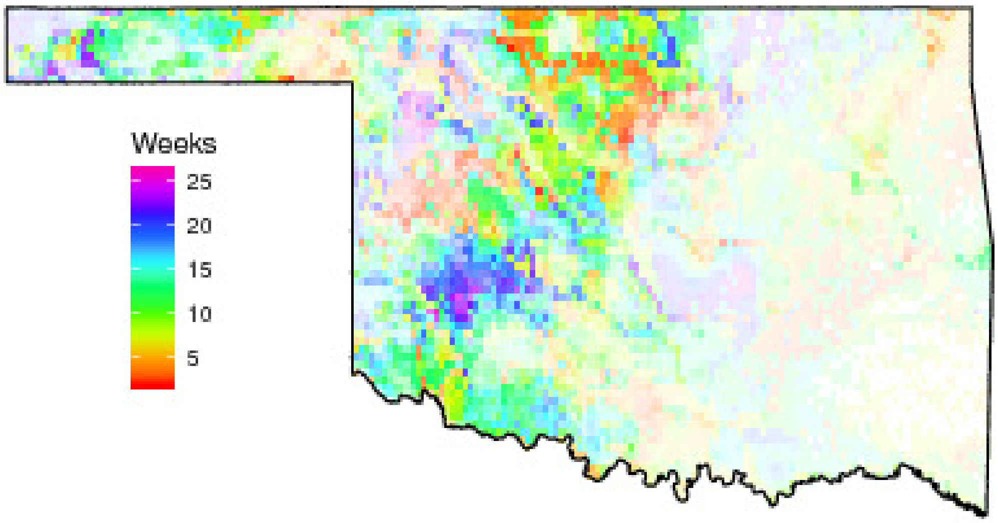

Figure 7: Average Weeks After Planting at which the interquartile range of forecasted yield percentile was less than 33% for Oklahoma for seasons 1997-2016

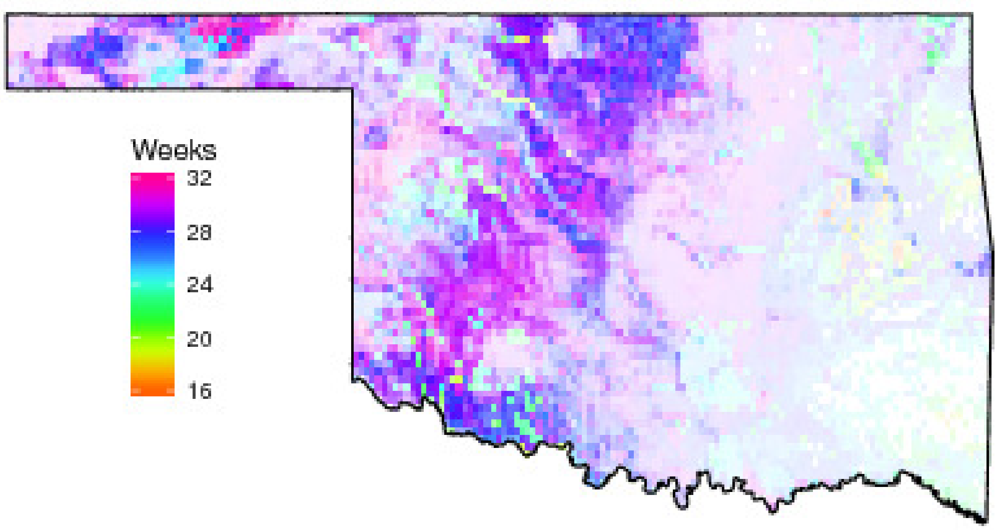

Figure 8: Average Weeks After Planting at which the interquartile range of forecasted yield percentile was less than 10% for Oklahoma for seasons 1997-2016

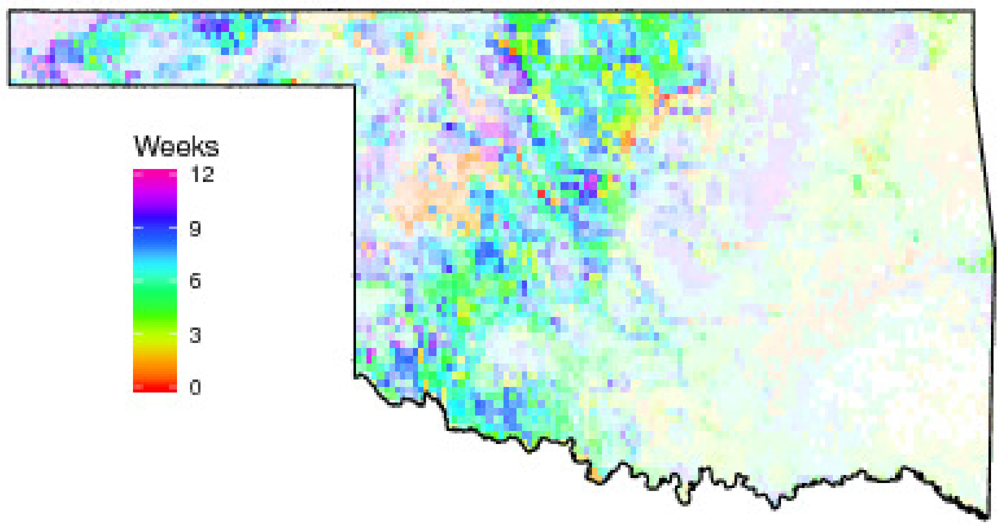

Figure 9: Standard deviation in annual variability of predicted week after planting at which the interquartile range of forecasted yield percentile was less than 33% for Oklahoma for seasons 1997-2016

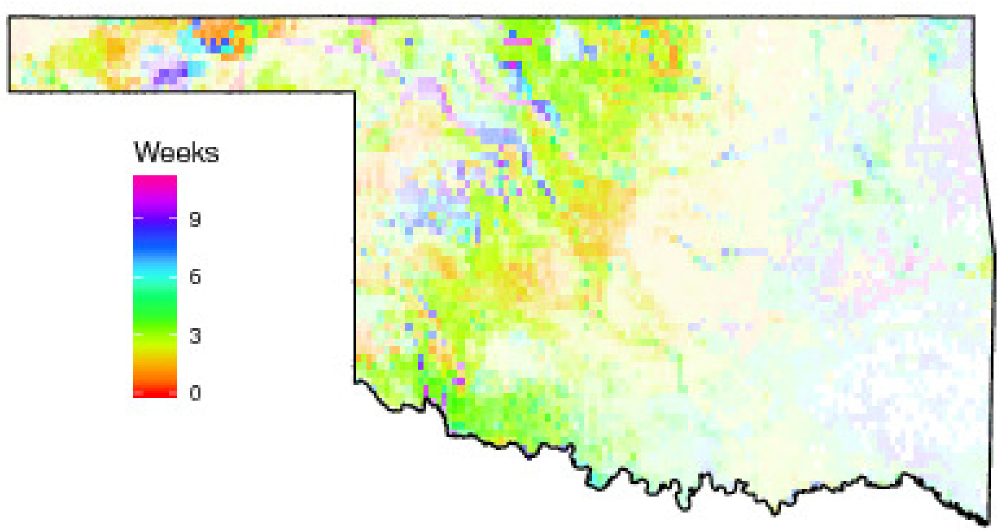

Figure 10: Standard deviation in annual variability of predicted week after planting at which the interquartile range of forecasted yield percentile was less than 10% for Oklahoma for seasons 1997-2016

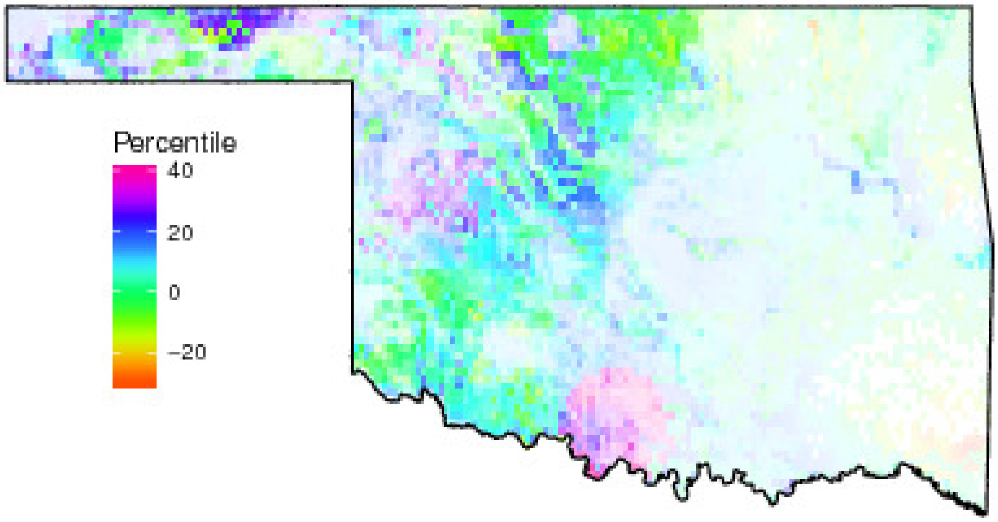

Figure 11: Average Percentile yield difference between initial condition set to 100% initial soil moisture and base simulation for the 1997-2016 seasons

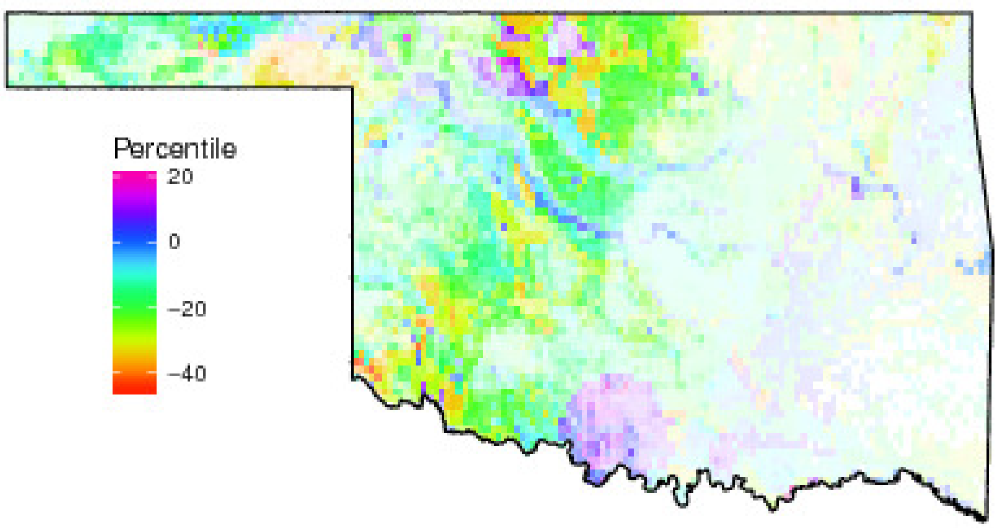

Figure 12: Average Percentile yield difference between initial condition set to 0% initial soil moisture and base simulation for the 1997-2016 seasons

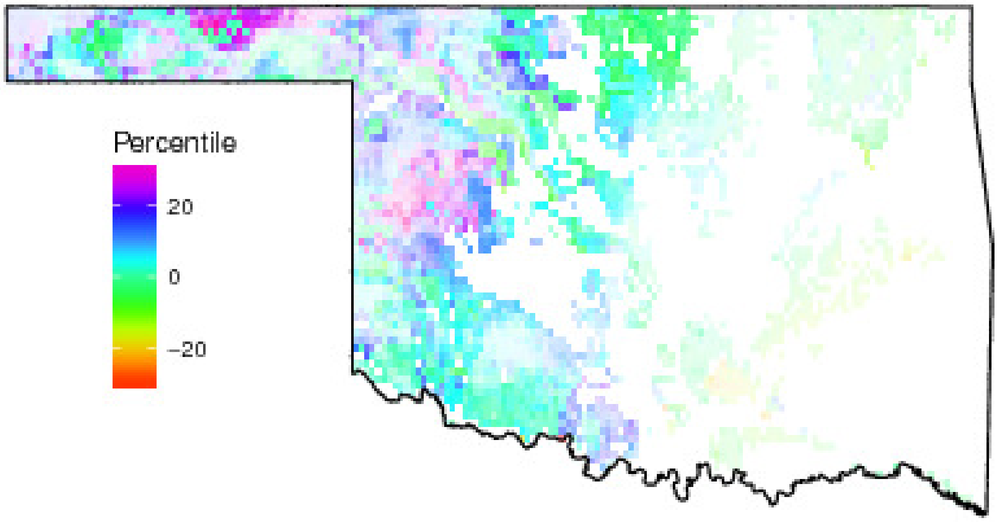

Figure 13: Average Percentile yield difference between initial condition set to Automatic Planting October and base simulation for the 1997-2016 seasons

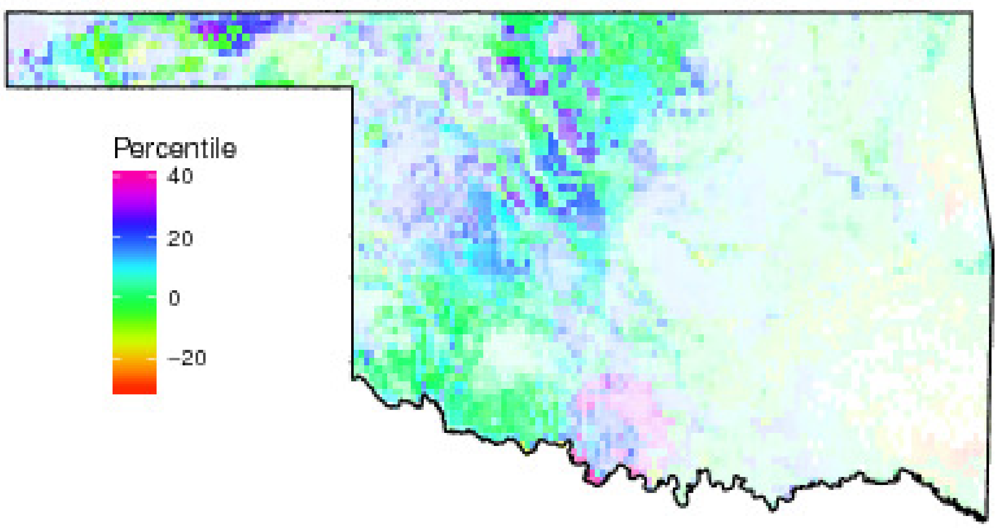

Figure 14: Average Percentile yield difference between initial condition set to Automatic Planting September and base simulation for the 1997-2016 seasons

CHAPTER III

ANALYSIS OF SPATIOTEMPORAL VARIABILITY IN IRRIGATION DEMAND FOR OKLAHOMA USING SIMULATION MODELING

Abstract

Agriculture accounts for close to 70% of the withdrawn used from surface water and ground water around the world (Wisser et al., 2008). Having the ability to forecast irrigation demand at a regional level is valuable for knowing how to allocate resources in the future. The objective of the study was to evaluate initial simulation conditions and data inputs for measuring irrigation demand in Oklahoma. Multiple simulations for corn and cotton were run using the Decision Support System for Agrotechnology Transfer – Cropping System Model (DSSAT-CSM) to see how the model responded to weather data, soil data, irrigation scheduling method, irrigation demand calculation method, and initial soil moisture. It was found the automatic irrigation scheduling method had a higher irrigation demand than the fixed irrigation scheduling method. Also, STATSGO2 soil data show more variability in irrigation demand than SoilGrids across Oklahoma. Allowing DSSAT to calculate irrigation demand resulted in higher estimations of irrigation demand than calculating irrigation demand by subtracting cumulative rain from evapotranspiration.

1. Introduction:

Irrigation demand is expected to increase in the future due to climate change (OWRB, 2011). Developing an accurate method of estimating regional irrigation demand is important for water resource planning. State agencies could apply irrigation demand estimates for permit applications. Viewing spatial characteristics, can help determine which areas of the state require the most attention in terms of drought risk, and aid in yearly planning. For example, having the ability to know which part of the state is more likely to experience a higher irrigation demand that year, will allow producers to prepare in advance by selecting a better crop, variety, or planting population suited to their location.

Numerous studies have explored methods to accurately predict irrigation water demand. Fant et al. (2012) used the CliCrop model to study world irrigation demand. They found that dry climates were predicted with more accuracy due to fewer rainfall events. They also compared the CliCrop model to DSSAT and noted the crop water requirements between the two models are similar. Satti and Jacobs (2004) developed at GIS-based Water Resources and Agricultural Permitting and Planning System by using the Agricultural Field Scale Irrigation Requirements Simulation crop model, and a data base management system within an ArcGIS framework. They found that while including soil heterogeneity is important to the water requirements of individual farms, regional water demands are adequately captured using the predominant soil type for each farm. Brumbelow and Georgakakos (2001) created a study to assess irrigation demand under climate changes in the U.S by using DSSAT-CSM. DSSAT was able to closely model the observed water balance throughout the growing season. They stated that DSSAT will provide a valid representation of the soil water balance as long it is initialized correctly. CROPGRO-Cotton and CERES-Maize are two crop models from the DSSAT-CSM modeling framework that have been used to estimate crop water demand. Thorp et al. (2015) used CSM-CROPGRO-Cotton to find irrigation requirements, and found the model was useful in identifying areas in a field that required more or less irrigation. Thorp et al. (2014) found CSM-CROPGRO-Cotton responded well to different management and climate change factors, including irrigation rates, N fertilization rates, and planting densities. Using DSSAT has limitations in some areas. Heinemann et al. (2002) performed a study to determine the irrigation requirements of crops in Brazil for maize, soybean, and dry bean. They noted a limitation of the DSSAT soil module's capability to describe water and nitrate movement from layer to layer. This was due to the cascading method DSSAT uses to calculate drainage. If drainage does not occur in 24 hours, there is a tendency to overestimate deep drainage and leaching, which could affect clay soils the most. Yang et al. (2010) used DSSAT and COTTON2K to estimate irrigation amounts for wheat, maize, cotton, vegetables, and fruit trees in Northern China. They noted the biggest challenge is the acquisition of sufficient soil input data, and they only used 10 soil profiles.

Little has been done for studying spatial temporal irrigation demand forecasting across Oklahoma or the Southern Great Plains. Past studies have shown that GIS has potential (Weatherhead and Knox, 2000; Satti and Jacobs, 2004; Santhi et al., 2005), but were limited in the amount and type of data to run the model. Utilizing tools such as the Oklahoma Mesonet, and NASA – Climate Hazards Group InfraRed Precipitation with Station data (NASA-CHIRPS) weather data, should present more accurate detail due to the high station population, and high spatial resolution, and frequency of data being acquired. The variation in precipitation across Oklahoma would be a good test for the models to determine if they perform well spatially across all climate zones. The models may demonstrate a better performance in certain climate zones. Examining the temporal aspect with the daily measured weather output could show times of the year where weather works more favorably for the models.

Objective

- Evaluate initial simulation conditions and data inputs for spatially quantifying irrigation demand in Oklahoma.

2. Materials and Methods:

2.1 Crop Models:

Decision Support System for Agrotechnology Transfer Cropping Systems Model (DSSAT-CSM; Jones et al., 2003) is a crop modeling system with multiple modules. CROPSIM-CERES Maize (Thorp et al., 2010) and CROPGRO Cotton (Boote et al., 1998) models are computer simulation models which incorporate crop management decisions such as planting date, fertilizer rate, and irrigation scheduling to simulate crop growth and development. Climate, soil, and cultivar parameters are the main inputs to run the model. The cultivar parameterization used for corn (Table 1) was from Araya et al. (2017), and the parameterization for cotton (Table 2) was from Modala et al. (2015). NASS (2010) listed usual planting dates for corn and cotton in Oklahoma, and the planting dates chosen for the simulations were in between the listed a typical early date and the typical late date for planting. Simulated planting date for corn was May 10th and for cotton was April 26th. Functions from the dssatR R package (Alderman, 2014) were used to build experiment files, soil files, and incorporate weather files using an R interface. Because DSSAT-CSM is a point-based model, an interface was written to allow the model to read and write data in Network Common Data Format (NetCDF), a widely-used gridded data format. To generate spatial output, the interface runs a simulation at every pixel in the study area and connects the pixels together. The interface was designed to be flexible to allow for gridded simulations at any resolution as determined by the input data.

2.2 Weather and Soil Data:

Variables used for simulation included daily maximum and minimum air temperature, cumulative daily solar radiation, and 2 meter average wind speed. The Oklahoma Mesonet, NASA-CHIRPS, and NOAA Stage IV QPE are different precipitation products that were used for the simulations. The Oklahoma Mesonet (McPherson et al., 2007) is a network of 121 automated environmental monitoring stations. There is at least one station per county in Oklahoma. Each station has a 10-meter tall tower, and environment observations are made every 5 minutes. For this study, daily summary data from the Mesonet were interpolated through Inverse Distance Weighting (IDW) using the R package gstat (Gräler et al., 2016). For this study, data were interpolated using a power value of 2 to create a nominally 5 km grid across Oklahoma. NOAA Stage IV QPE (Lin and Mitchell, 2005) provides hourly rainfall data based off multi-sensor analysis which were aggregated to daily rainfall totals. CHIRPS (Funk et al., 2014) is precipitation data which creates gridded rainfall time series precipitation data by incorporating satellite imagery with on ground station data. CHIRPS data has a 30 year time-span and on a 5 km spatial resolution.

Soil type for each 5 km grid box was selected as the soil type with the largest areal coverage within the grid box. Soil data were derived from STATSGO2 and Soilgrids. Soilgrids (ISRIC, 2013) is a soil database created by collecting soil samples and then using a model to estimate soil types and properties with global coverage at a 250 m resolution. STATSGO2 (Soil Survey Staff, 2017) is the Digital General Soil Map of the United States which estimates soil types based on landscape and is displayed at a scale of 1:250,000 (Staff, 2016). For both Soilgrids and STATSGO2, soil lower limit (SLLL), drained upper limit (SDUL), and saturated soil moisture (SSAT) were set to values of soil moisture at -1500, -30, and 0 kpa, respectively. Missing values for these variables were estimated using nearest neighbor analysis based on soil texture and saturated conductivity. Runoff curve number was estimated using hydrologic soil group (HSG) and slope. Missing HSG values were estimated using soil depth and saturated conductivity based on NRCS (2004). Values for soil drainage rate (SLDR) parameter were estimated using the drainage class from STATSGO2 and the get.sldr function from dssatR (Alderman, 2014). For missing drainage class values SLDR was assumed to be 0.6. Values for Soil nitrogen mineralization factor (FLNI) and soil productivity factor (SLPF) were both set to 1.0.

2.3 Model Configuration Testing:

Several simulations were created to investigate the possible outcomes of DSSAT-CSM when estimating irrigation demand. The simulations were run for each year, 1998-2016 with varying configurations. Four simulation files were created for corn and cotton and then tested with different soil data, precipitation data, and initial soil moisture values. The conditions for the system files are outlined in Table 3, and the configurations for each system file are outlined in Table 4. Two simulations used a spin-up of 10 days after harvest of the previous season. All simulations without spin-up have a simulation start date 10 days prior to planting. Automatic irrigation can be applied in two ways in DSSAT. One way was to allow DSSAT to fully irrigate the crop whenever it needed water, and is referred to as fully irrigated. The other way was to apply a fixed 6mm amount of irrigation water per application, and is referred to as fixed irrigation. The assumption of applying 6mm of irrigation water for fixed irrigation was estimated by looking at general water well outputs in typical irrigated areas in Oklahoma. The water well outputs were found on the Oklahoma Water Resource Board (OWRB) website. Irrigation demand was calculated two ways. One way was by letting DSSAT calculate irrigation demand, and the other was to subtract rainfall from reference ET.

3. Results:

In general, irrigation demand was less in Eastern Oklahoma and higher in the western part of the state with the Panhandle having the highest irrigation demand. As one might expect, simulations with 0% initial soil moisture required more water than simulations with 100% initial soil moisture. The simulations with spin-up helped offset the soil moisture deficit or surplus when the models were configured with 100% and 0% initial soil moisture.

Figure 2 shows the mean annual irrigation demand for fully irrigated corn calculated by DSSAT's cumulative irrigation output with initial soil moisture set at 50% for the 1998-2016 seasons. Figure 2a is using STATSGO2 soil data, and figure 2b is using Soilgrids soil data. STATSGO2 soil data shows more diversity in irrigation demand than soilgrids. Soilgrids still shows the expected west to east trend of decreasing irrigation demand, but does not pick up on the finer details. Figures 3-10 for the mean and standard deviation of annual irrigation demand used STATSGO2 soil data with initial soil moisture at 50%, and simulated across the 1998-2016 seasons.

Overall, irrigation demand was higher when calculating irrigation demand using DSSAT than ET-rain because the ET-rain calculation does not include irrigation efficiency. Figure 3 shows the mean annual irrigation demand for corn calculated by DSSAT's cumulative irrigation output. Figure 3a shows irrigation demand using full irrigation without spin-up. Figure 3b shows irrigation demand using full irrigation with spin-up. Figure 3c shows irrigation demand using fixed irrigation without spin-up. Figure 3d shows irrigation demand using fixed irrigation with spin-up. Figures 3a and 3b show that irrigation demand is estimated higher on average when setting the simulation to full irrigation. Figures 3a and 3b seem to be about 200 mm higher across the state compared to figures 3c and 3d. Figures 3b and 3d show the effect of spin-up. There was little difference between simulations with spin-up and simulations without spin-up. Using either fixed or full irrigation had little effect on the spatial distribution of irrigation demand. Figures 3a and 3b show the same spatial distribution of irrigation demand as figures 3c and 3d. Figure 4 shows the mean annual irrigation demand for corn calculated by subtracting rain from ET. Figure 4a shows irrigation demand using full irrigation without spin-up. Figure 4b shows irrigation demand using full irrigation with spin-up. Figure 4c shows irrigation demand using fixed irrigation without spin-up. Figure 4d shows irrigation demand using fixed irrigation with spin-up. The simulations with the full irrigation treatment (figures 4a,b), are 100 mm higher than the simulations under fixed irrigation (figures 4c,d). Simulations with spin-up (Fig. 4b,d), use about 100 mm less irrigation water than simulations with out spin-up (Fig. 4a,c). The spatial pattern between the simulations is similar. Overall, figure 4 shows about 200 mm less irrigation water being used than figure 3. The effect of spin-up is about 50 to 100 mm larger in figure 4 than in figure 3.

The results for cotton are very similar to the results for corn. However, cotton used less irrigation water than corn. Figure5 shows the mean annual irrigation demand for cotton calculated by DSSAT's cumulative irrigation output. Figure 5a shows irrigation demand using full irrigation without spin-up. Figure 5b shows irrigation demand using full irrigation with spin-up. Figure 5c shows irrigation demand using fixed irrigation without spin-up. Figure 5d shows irrigation demand using fixed irrigation with spin-up. Comparing figures 5a and 5b to figures 5c and 5d, show that irrigation demand is estimated higher when setting the simulation to full irrigation. Irrigation demand under full irrigation seems to be about 100 mm higher across the state compared to simulations with fixed irrigation. Simulations with spin-up used around 100 mm less irrigation water than simulations without spin-up. Using either fixed or full irrigation had little effect on the spatial distribution of irrigation demand. Figures 5a and 5b show the same spatial distribution of irrigation demand as figures 5c and 5d. Figure 6 shows the mean annual irrigation demand for cotton calculated by subtracting rain from ET. Figure 6a shows irrigation demand using full irrigation without spin-up. Figure 6b shows irrigation demand using full irrigation with spin-up. Figure 6c shows irrigation demand using fixed irrigation without spin-up. Figure 6d shows irrigation demand using fixed irrigation with spin-up. The simulations with the full irrigation treatment (figures 6a,b), are 50 to 100 mm higher than the simulations under fixed irrigation (figures 6c,d). Simulations with spin-up (Fig. 6b,d), use about 50 to 100 mm less irrigation water than simulations without spin-up (Fig. 6a,c). The spatial pattern between the simulations are similar. Overall, figure 6 shows about 100 mm less irrigation water being used than figure 6. The effect of spin-up is about 50 to 100 mm larger in figure 6 than in figure 5.

The standard deviations in annual irrigation demand were similar for both corn and cotton. Figure 7 shows the standard deviation in annual irrigation demand for corn calculated by DSSAT's cumulative irrigation output. Figure 7a shows irrigation demand using full irrigation without spin-up. Figure 7b shows irrigation demand using full irrigation with spin-up. Figure 7c shows irrigation demand using fixed irrigation without spin-up. Figure 7d shows irrigation demand using fixed irrigation with spin-up. The standard deviation in annual water use was 100 mm less across the state using fix irrigation instead of full irrigation. Using spin-up in a simulation increased the standard deviation. Figure 8 shows the standard deviation in annual irrigation demand for corn calculated by subtracting rain from ET. Figure 8a shows irrigation demand using full irrigation without spin-up. Figure 8b shows irrigation demand using full irrigation with spin-up. Figure 8c shows irrigation demand using fixed irrigation without spin-up. Figure 8d shows irrigation demand using fixed irrigation with spin-up. Same as figure 7, figure 8 shows the increase in standard deviation when spin-up is used. However, the difference between full and fixed irrigation is not as dramatic in figure 8 as in figure 7. Figure 9 shows the standard deviation in annual irrigation demand for cotton calculated by DSSAT's cumulative irrigation output. Figure 9a shows irrigation demand using full irrigation without spin-up. Figure 9b shows irrigation demand using full irrigation with spin-up. Figure 9c shows irrigation demand using fixed irrigation without spin-up. Figure 9d shows irrigation demand using fixed irrigation with spin-up. The simulations with spin-up (Fig.9b,d) had a higher standard deviation across the state than the simulation without spin-up (Fig. 9a,c). The fully irrigated simulations (Fig. 9a,b) have a standard deviation twice as high was the fixed irrigation simulations (Fig. 9c,d). Figure 10 shows the standard deviation in annual irrigation demand for cotton calculated by subtracting rain from ET. Figure 10a shows irrigation demand using full irrigation without spin-up. Figure 10b shows irrigation demand using full irrigation with spin-up. Figure 10c shows irrigation demand using fixed irrigation without spin-up. Figure 10d shows irrigation demand using fixed irrigation with spin-up. The fully irrigated simulations (Fig. 10a,b) had a higher standard deviation than the fixed irrigated simulations (Fig. 10c,d). However, the difference in standard deviation between fix and full irrigation was higher when calculated using DSSAT's cumulative irrigation output (Fig.9). The effect of spin-up is more drastic when calculating irrigation demand by ET-rain. The simulations with spin-up (Fig. 10b,d) are close to 50mm higher than the simulations without spin-up (Fig. 10a,c).

4. Discussion:

DSSAT is able to recognize general spatial trends in irrigation demand. Case in point, DSSAT recognized the east to west pattern of increasing irrigation demand in Oklahoma, and the anticipated result of 0% initial soil moisture simulations requiring more irrigation water than simulations with 100% initial soil moisture. This sensitivity to soil moisture adds to Dokoohaki et al. (2016) who studied the soil water balance of DSSAT and found the model to perform well overall when estimating soil water. It is important to include for future research that they did mention problems with the soil water balance model, and noted that soil–water evaporation, root water uptake, and deep percolation could have an effect on the total accuracy of the model. The simulations with a spin-up period were more useful when starting at 0 or 100 percent soil moisture than at 50% soil moisture. That is because there is not a major surplus or deficit the model must account for before the simulation starts. STATSGO2 was the better performer when it came to soil data. The reason why Soilgrids didn't show the same irrigation demand as STATSGO2 was Soilgrids assumes a uniform depth of 200 cm for most of Oklahoma, and missed the areas of the state where shallow soils exist. The soil depths in STATSGO2 varied across the state and generally picked up on areas with more shallow soils.

The results for mean annual irrigation demand between cotton and corn were very similar except cotton used less water than corn in each simulation scenario. The simulations where irrigation demand was calculated as a difference of ET and rain were lower for both corn and cotton. This could be due to irrigation efficiency not being accounted for in the ET-rain calculation. If the ET-rain calculations included water leaving through the soil, the estimated irrigation demand would be higher (Pereira et al., 2002). However, DSSAT estimated irrigation demand takes into account the soil water balance which is why the irrigation demand was estimated higher when calculated by DSSAT. There was a difference between the fully irrigated and fixed irrigated simulations in both the ET-rain and DSSAT calculated irrigation demand. This difference could be due to the fact the crop was more stressed under a fixed irrigation schedule than in a fully irrigated schedule, and because the fixed irrigated crop had a water deficit, it used less water (Fereres and Soriano, 2006). The standard deviation in annual irrigation demand between cotton and corn were similar. Using spin-up actually increased the standard deviation in irrigation demand for all simulations. This could be due the variability in precipitation between simulation start and planting. When letting DSSAT calculate irrigation demand, the standard deviation was almost twice as high compared to the fixed irrigation treatment, but when calculated by the ET-rain method they were close to each other. This could be caused by how the DSSAT model uses more variables to calculate irrigation demand than just subtracting rain from ET causing more annual variability.

5. Conclusion:

DSSAT can be used to estimate irrigation demand in Oklahoma. Setting up the experiments in different ways can provide dramatically different results such as using fixed or fully irrigated simulations. Also calculating irrigation demand by ET-rain or letting DSSAT do the calculating. Using STATSGO2 soil data was the better soil data set to use because it is able to identify areas where soils are more shallow. Where SoilGrids assumed a 2 m depth for almost all of Oklahoma. Soil moisture seemed to not matter as much when a spin-up period was used because the soil moisture had time to balance out before planting.

REFERENCES

Alderman, P. D. (2014), *dssatR: R interface to DSSAT-CSM models*.

Araya, A., I. Kisekka, P. H. Gowda, and P. V. Prasad (2017), Evaluation of water-limited cropping systems in a semi-arid climate using DSSAT-CSM, *Agricultural Systems*, *150*, 86–98.

Boote, K. J., J. W. Jones, and G. Hoogenboom (1998), Simulation of crop growth: CROPGRO model. In: Robert M. Peart and R. Bruce Curry, editors, Agricultural Systems Modeling and Simulation. Marcel Dekker, INC., New York, New York. p. 652-692

Brock, F. V., K. C. Crawford, R. L. Elliott, G. W. Cuperus, S. J. Stadler, H. L. Johnson, and M. D. Eilts (1995), The Oklahoma Mesonet: A technical overview, *Journal of Atmospheric and Oceanic Technology*, *12*(1), 5–19.

Brumbelow, K., and A. Georgakakos (2001), An assessment of irrigation needs and crop yield for the United States under potential climate changes, *Journal of Geophysical Research: Atmospheres*, *106*(D21), 27383–27405.

Dokoohaki, H., M. Gheysari, S.-F. Mousavi, S. Zand-Parsa, F. E. Miguez, S. V. Archontoulis, and G. Hoogenboom (2016), Coupling and testing a new soil water module in DSSAT CERES-Maize model for maize production under semi-arid condition, *Agricultural Water Management*, *163*, 90–99.

Fant, C., A. Gueneau, K. Strzepek, S. Awadalla, W. Farmer, E. Blanc, and C. A. Schlosser (2012), *CliCrop: A crop water-stress and irrigation demand model for an integrated global assessment model approach*, MIT Joint Program on the Science; Policy of Global Change.

Fereres, E., and M. A. Soriano (2006), Deficit irrigation for reducing agricultural water use, *Journal of Experimental Botany*, *58*(2), 147–159.

Funk, C. C., P. J. Peterson, M. F. Landsfeld, D. H. Pedreros, J. P. Verdin, J. D. Rowland, B. E. Romero, G. J. Husak, J. C. Michaelsen, A. P. Verdin, and others (2014), A quasi-global precipitation time series for drought monitoring, *US Geological Survey Data Series*, *832*(4).

Gräler, B., E. Pebesma, and G. Heuvelink (2016), Spatio-temporal interpolation using gstat, *The R Journal*, *8*(1), 204–218.

Heinemann, A., G. Hoogenboom, and R. De Faria (2002), Determination of spatial water requirements at county and regional levels using crop models and GIS: An example for the state of Parana, Brazil, *Agricultural Water Management*, *52*(3), 177–196.

Hengl, T., J. M. de Jesus, G. B. Heuvelink, M. R. Gonzalez, M. Kilibarda, A. Blagotić, W. Shangguan, M. N. Wright, X. Geng, B. Bauer-Marschallinger, and others (2017), SoilGrids250m: Global gridded soil information based on machine learning, *PLoS One*, *12*(2), e0169748.

ISRIC (2013), SoilGrids: An automated system for global soil mapping,

Jones, J. W., G. Hoogenboom, C. H. Porter, K. J. Boote, W. D. Batchelor, L. Hunt, P. W. Wilkens, U. Singh, A. J. Gijsman, and J. T. Ritchie (2003), The DSSAT cropping system model, *European Journal of Agronomy*, *18*(3), 235–265.

Lin, Y., and K. E. Mitchell (2005), 1.2 the ncep stage ii/iv hourly precipitation analyses: Development and applications, in *19th Conf. Hydrology*, Citeseer.

McPherson, R. A., C. A. Fiebrich, K. C. Crawford, J. R. Kilby, D. L. Grimsley, J. E. Martinez, J. B. Basara, B. G. Illston, D. A. Morris, K. A. Kloesel, and others (2007), Statewide monitoring of the mesoscale environment: A technical update on the Oklahoma Mesonet, *Journal of Atmospheric and Oceanic Technology*, *24*(3), 301–321.

Modala, N. R., S. Ale, N. Rajan, C. L. Munster, P. B. DeLaune, K. R. Thorp, S. S. Nair, and E. M. Barnes (2015), Evaluation of the csm-cropgro-cotton model for the Texas rolling plains region and simulation of deficit irrigation strategies for increasing water use efficiency, *Transactions of the ASAE*, *58*(3), 685–696.

NRCS (2004), National engineering handbook: Part 630—Hydrology, *USDA Soil Conservation Service: Washington, DC, USA*.

OWRB (2011), Oklahoma comprehensive water plan 2012 update: Water demand forecast report,

Pereira, L. S., T. Oweis, and A. Zairi (2002), Irrigation management under water scarcity, *Agricultural Water Management*, *57*(3), 175–206.

Santhi, C., R. Muttiah, J. Arnold, and R. Srinivasan (2005), A GIS-based regional planning tool for irrigation demand assessment and savings using SWAT, *Transactions of the ASAE*, *48*(1), 137–147.

Satti, S. R., and J. M. Jacobs (2004), A GIS-based model to estimate the regionally distributed drought water demand, *Agricultural Water Management*, *66*(1), 1–13.

Soil Survey Staff (2017), *Web Soil Survey*, Natural Resources Conservation Service, United States Department of Agriculture.

Staff, S. S. (2016), Natural resources conservation service, United States Department of Agriculture. US General Soil Map (STATSGO2),

Thorp, K., D. Hunsaker, A. French, E. Bautista, and K. Bronson (2015), Integrating geospatial data and cropping system simulation within a geographic information system to analyze spatial seed cotton yield, water use, and irrigation requirements, *Precision Agriculture*, *16*(5), 532–557.

Thorp, K. R., D. J. Hunsaker, A. N. French, J. W. White, T. R. Clarke, and P. J. Pinter Jr (2010), Evaluation of the CSM-CROPSIM-CERES-Wheat model as a tool for crop water management, *Transactions of the ASABE*, *53*(1), 87–102.

Thorp, K. R., E. M. Barnes, D. J. Hunsaker, B. A. Kimball, J. W. White, V. J. Nazareth, and G. Hoogenboom (2014), Evaluation of CSM-CROPGRO-Cotton for simulating effects of management and climate change on cotton growth and evapotranspiration in an arid environment, *Transactions of the ASABE*, *57*(6), 1627–1642.

Weatherhead, E., and J. Knox (2000), Predicting and mapping the future demand for irrigation water in england and wales, *Agricultural Water Management*, *43*(2), 203–218.

Wisser, D., S. Frolking, E. M. Douglas, B. M. Fekete, C. J. Vörösmarty, and A. H. Schumann (2008), Global irrigation water demand: Variability and uncertainties arising from agricultural and climate data sets, *Geophysical Research Letters*, *35*(24).

Yang, Y., Y. Yang, J. P. Moiwo, and Y. Hu (2010), Estimation of irrigation requirement for sustainable water resources reallocation in north china, *Agricultural Water Management*, *97*(11), 1711–1721.

Table 1: Corn Parameters

Parameter	Description	Value
P1	Emergence to end of juvenile phase (in degree days)	230
P2	The extent to which development is delayed for each hour increase in photoperiod above the longest photoperiod at which development proceeds at max. rate	0.78
P5	Degree days silking to physiological maturity	990
G2	Maximum number of kernels per plant	920.4
G3	Kernel filling rate during the linear grain filling stage and under optimum condition (mg/day)	7.3
PHINT	Phylochron interval (degree days)	65.9

Table 2: Cotton parameters

Parameter	Description	Value
PL-EM	Time between planting and emergence	3
FL-LF	Time between first flower and end of main stem	50
FL-VS	Time from first flower to last leaf of main stem	45
LFMAX	Maximum leaf photosynthesis rate	1.7
RHGHT	Relative height of the ecotype in comparison to the standard height per node (YVSHT)	0.6
RWDTH	Relative width of the ecotype in comparison to the standard width per node (YVSWH)	0.35
TRIFL	Rate of appearance of leaves on the main stem	0.3
YHWTEM	Effect of temperature on the length of each internode	0.01, 0.02, 0.43, 0.85, and 0.85
SLAVR	Specific leaf area of cultivar under standard growth conditions	130
XFRT	Maximum fraction of daily growth that is partitioned to seed + shell	0.75
SFDUR	Seed filling duration for pod cohort at standard growth conditions	30
LNGSH	Time required for growth of individual shells	14
XVSHT	Number of nodes on main stem	0, 1, 10, 10, 16, 18, 20, 24, and 25

Table 3: Filex configurations

Crop	Automatic Irrigation Method	Spin-up
Corn	Full	No
Corn	Full	Yes
Corn	Fixed	No
Corn	Fixed	Yes
Cotton	Full	No
Cotton	Full	Yes
Cotton	Fixed	No
Cotton	Fixed	Yes

Table 4: Simulation configurations

Soil	Weather	Soil Moisture (%)
STATSGO2	IDW Mesonet	0
STATSGO2	IDW Mesonet	50
STATSGO2	IDW Mesonet	100
STATSGO2	CHIRPS	0
STATSGO2	CHIRPS	50
STATSGO2	CHIRPS	100
STATSGO2	NOAA	0
STATSGO2	NOAA	50
STATSGO2	NOAA	100
SoilGrids	IDW Mesonet	0
SoilGrids	IDW Mesonet	50
SoilGrids	IDW Mesonet	100
SoilGrids	CHIRPS	0
SoilGrids	CHIRPS	50
SoilGrids	CHIRPS	100
SoilGrids	NOAA	0
SoilGrids	NOAA	50
SoilGrids	NOAA	100

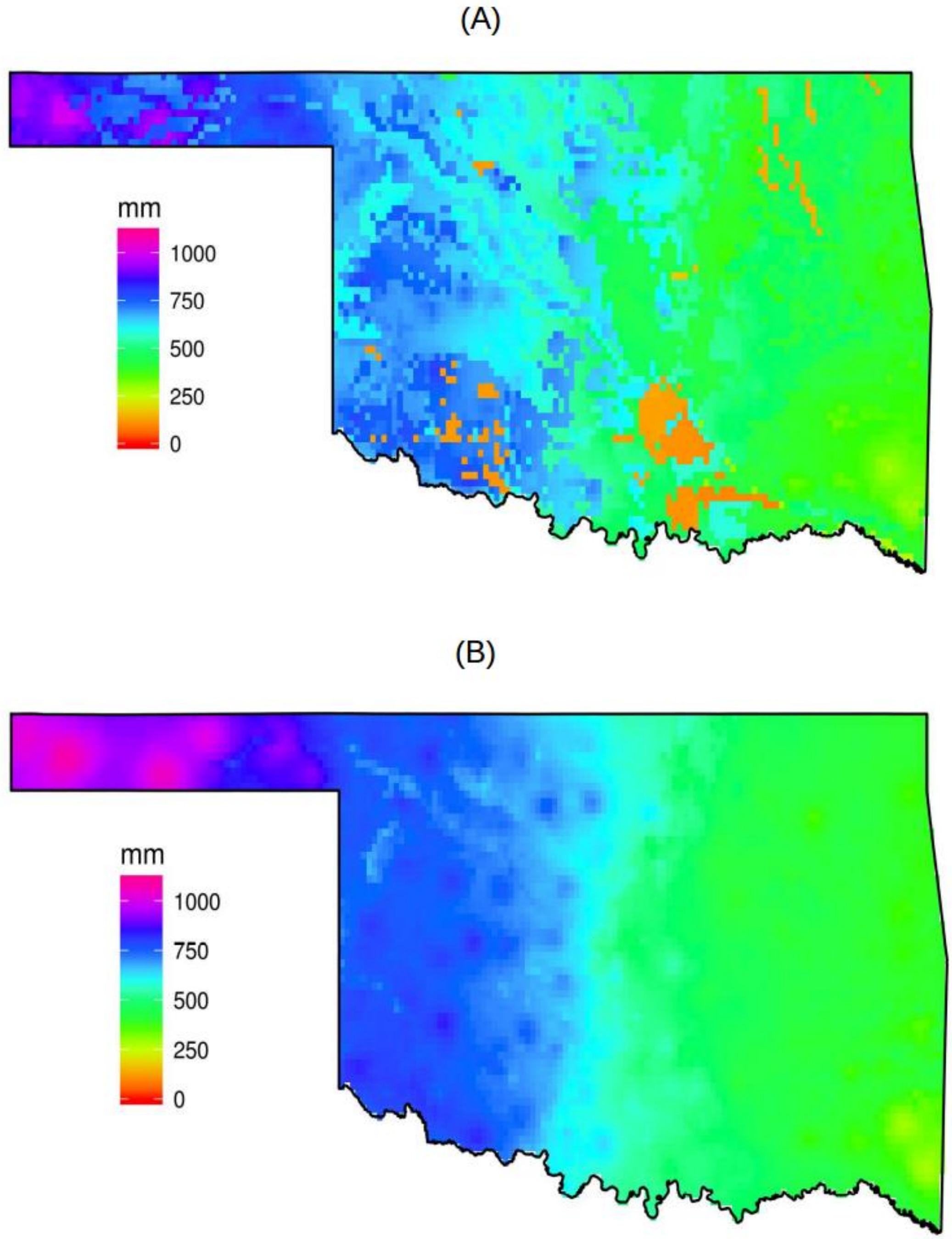

Figure1: (A) STATSGO2 soil data. (B) SoilGrids soil data. Both figures are simulations used 50 soil moisture with irrigation demand calculated by DSSAT.

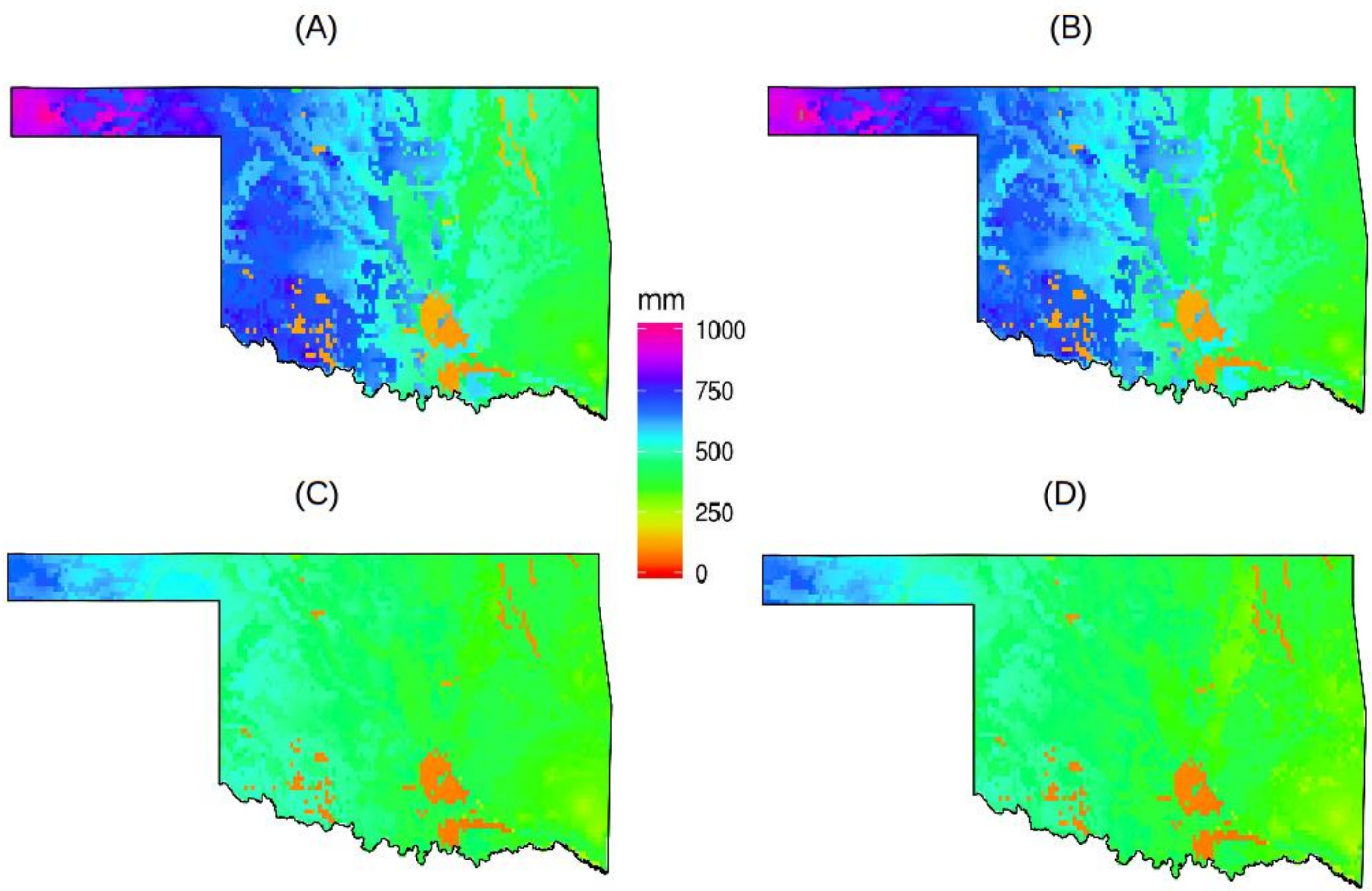

Figure 2: (A) Mean annual irrigation demand for corn with simulation starting 10 days before planting using STATSGO2 soil data at 50% initial soil moisture. (B) Mean annual irrigation demand for corn with simulation starting 10 days after harvest using STATSGO2 soil data at 50% initial soil moisture. (C) Mean annual irrigation demand for corn with simulation starting 10 days before planting using STATSGO2 at 50% initial soil moisture. Irrigation demand in calculated using a fixed amount of 6 mm per applications. (D) Mean annual irrigation demand for corn with simulation starting 10 days after harvest using STATSGO2 at 50% initial soil moisture. Irrigation demand in calculated using a fixed amount of 6 mm per applications

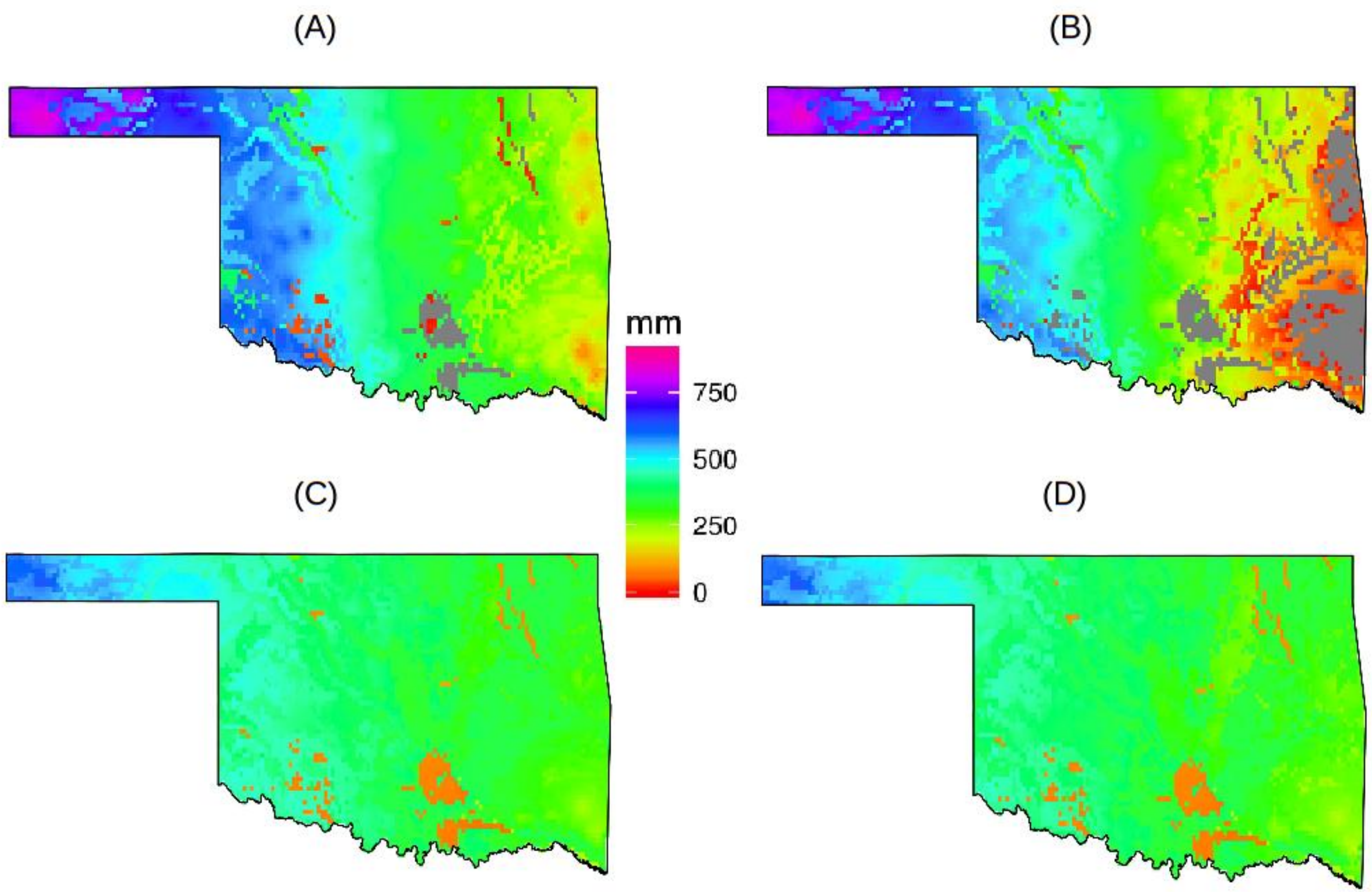

Figure 3: (A) Mean annual irrigation demand for corn with simulation starting 10 days before planting using STATSGO2 soil data at 50% initial soil moisture. Irrigation demand calculated by subtracting ET from rainfall. (B) Mean annual irrigation demand for corn with simulation starting 10 days after harvest using STATSGO2 soil data at 50% initial soil moisture. Irrigation demand calculated by subtracting ET from rainfall. (C) Mean annual irrigation demand for corn with simulation starting 10 days before planting using STATSGO2 at 50% initial soil moisture. Irrigation demand in calculated using a fixed amount of 6 mm per applications. Irrigation demand calculated by subtracting ET from rainfall. (D) Mean annual irrigation demand for corn with simulation starting 10 days after harvest using STATSGO2 at 50% initial soil moisture. Irrigation demand in calculated using a fixed amount of 6 mm per applications. Irrigation demand calculated by subtracting ET from rainfall.

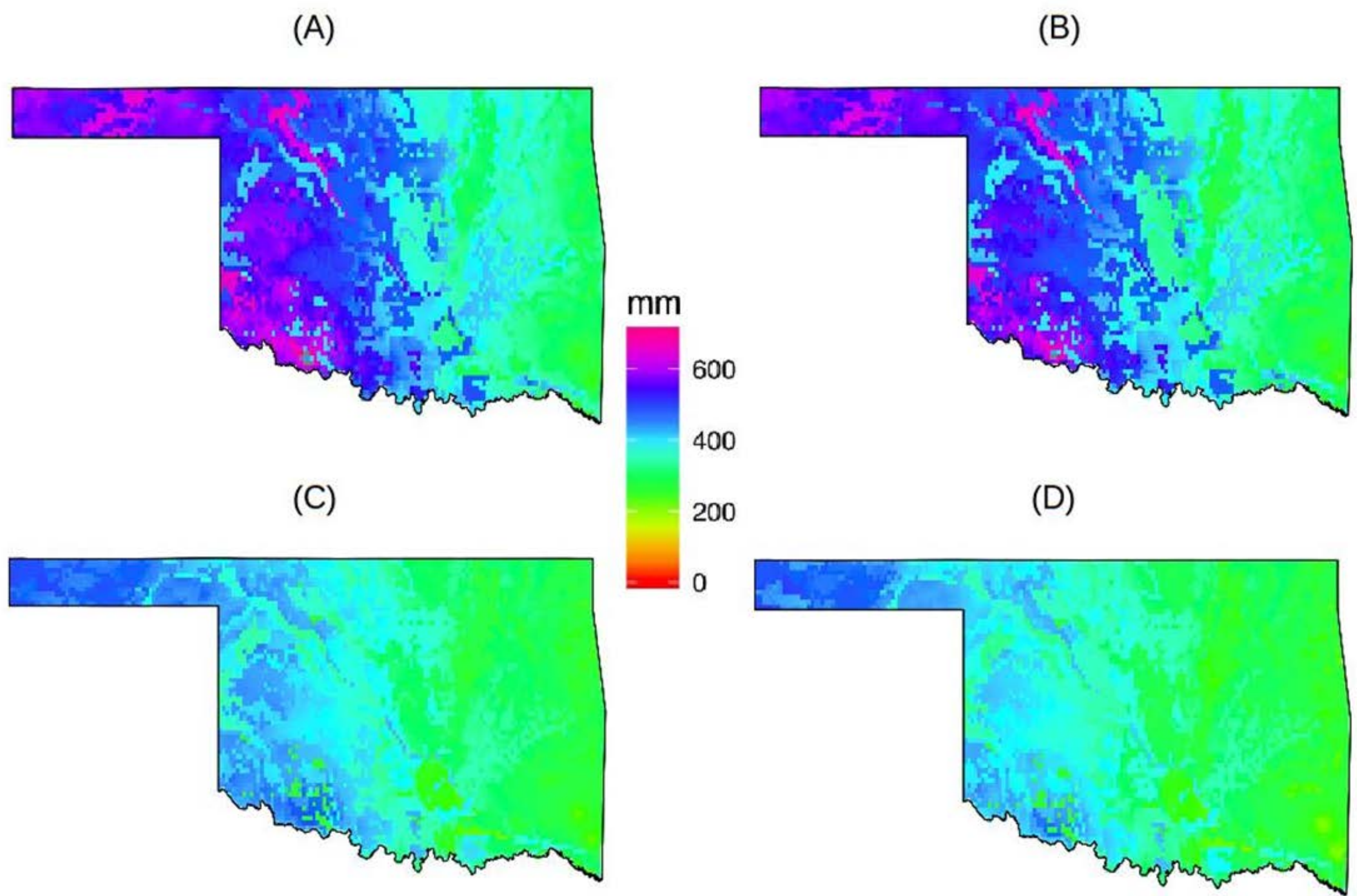

Figure 4: (A) Mean annual irrigation demand for cotton with simulation starting 10 days before planting using STATSGO2 soil data at 50% initial soil moisture. (B) Mean annual irrigation demand for cotton with simulation starting 10 days after harvest using STATSGO2 soil data at 50% initial soil moisture. (C) Mean annual irrigation demand for cotton with simulation starting 10 days before planting using STATSGO2 at 50% initial soil moisture. Irrigation demand in calculated using a fixed amount of 6 mm per applications. (D) Mean annual irrigation demand for cotton with simulation starting 10 days after harvest using STATSGO2 at 50% initial soil moisture. Irrigation demand in calculated using a fixed amount of 6 mm per applications

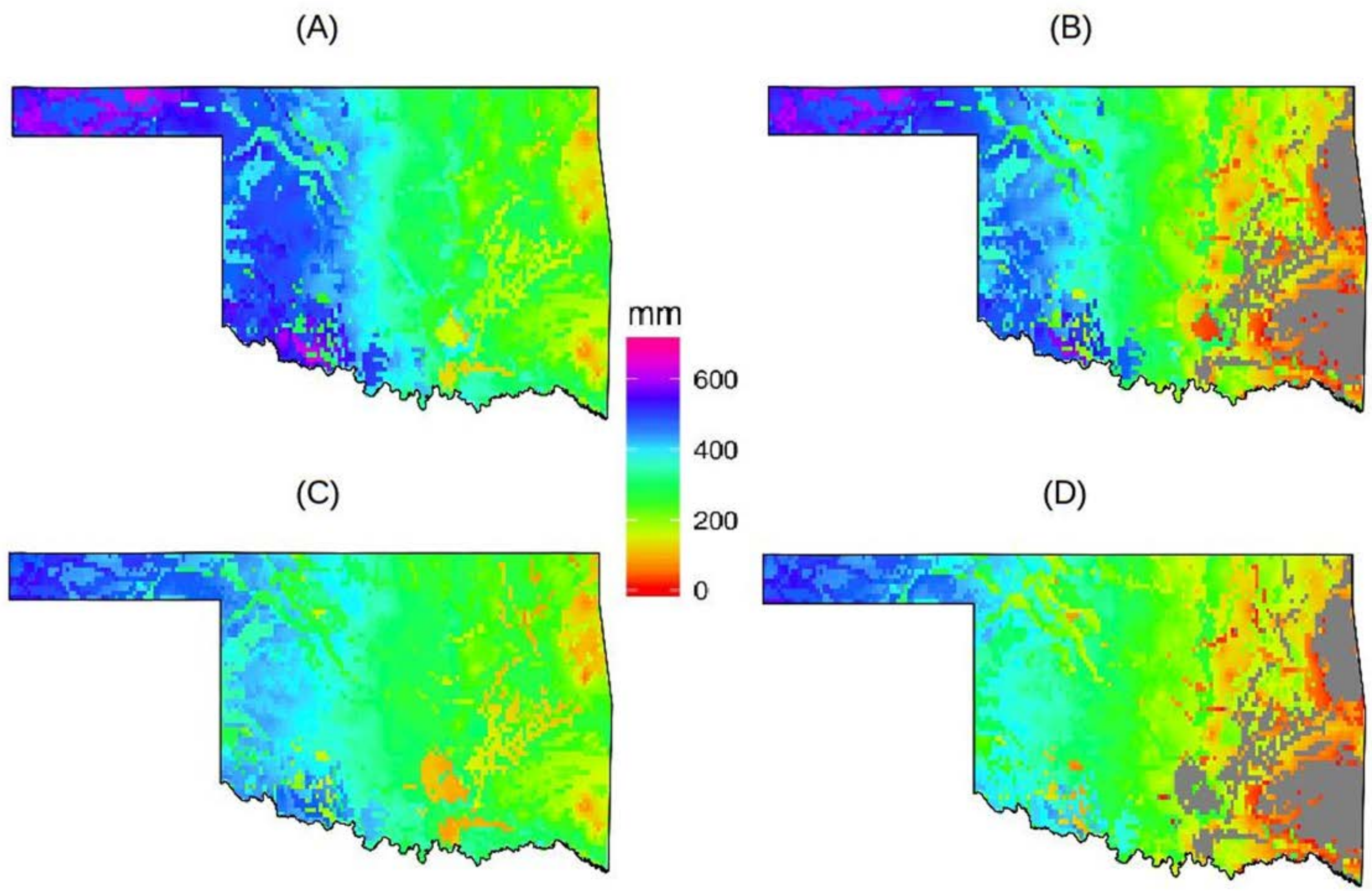

Figure 5: (A) Mean annual irrigation demand for cotton with simulation starting 10 days before planting using STATSGO2 soil data at 50% initial soil moisture. Irrigation demand calculated by subtracting ET from rainfall. (B) Mean annual irrigation demand for cotton with simulation starting 10 days after harvest using STATSGO2 soil data at 50% initial soil moisture. Irrigation demand calculated by subtracting ET from rainfall. (C) Mean annual irrigation demand for cotton with simulation starting 10 days before planting using STATSGO2 at 50% initial soil moisture. Irrigation demand in calculated using a fixed amount of 6 mm per applications. Irrigation demand calculated by subtracting ET from rainfall. (D) Mean annual irrigation demand for cotton with simulation starting 10 days after harvest using STATSGO2 at 50% initial soil moisture. Irrigation demand in calculated using a fixed amount of 6 mm per applications. Irrigation demand calculated by subtracting ET from rainfall.

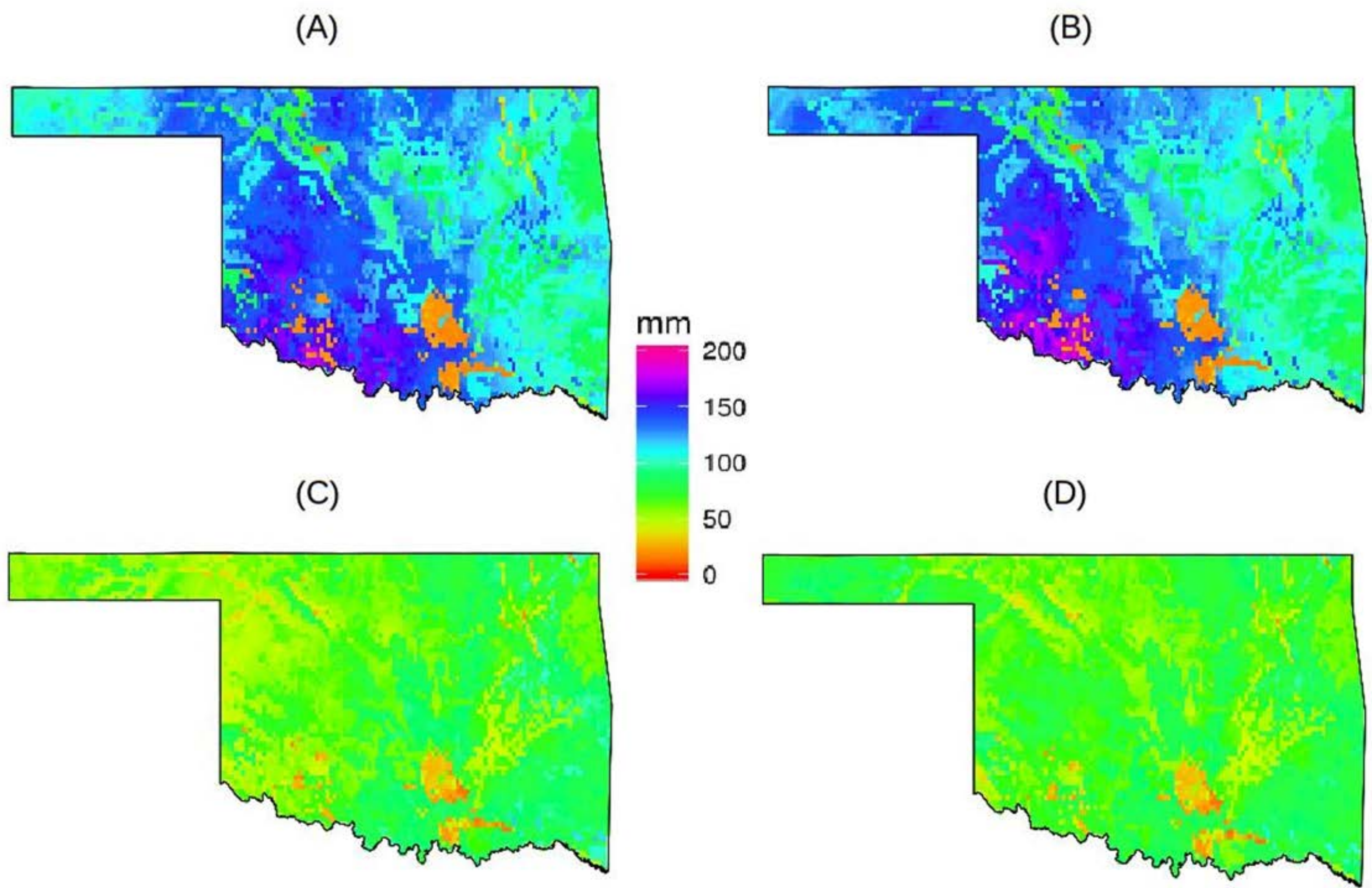

Figure 6: (A) Standard deviation in annual irrigation demand for corn with simulation starting 10 days before planting using STATSGO2 soil data at 50% initial soil moisture. (B) Standard deviation in annual irrigation demand for corn with simulation starting 10 days after harvest using STATSGO2 soil data at 50% initial soil moisture. (C) Standard deviation in annual irrigation demand for corn with simulation starting 10 days before planting using STATSGO2 at 50% initial soil moisture. Irrigation demand in calculated using a fixed amount of 6 mm per applications. (D) Standard deviation in annual irrigation demand for corn with simulation starting 10 days after harvest using STATSGO2 at 50% initial soil moisture. Irrigation demand in calculated using a fixed amount of 6 mm per applications.

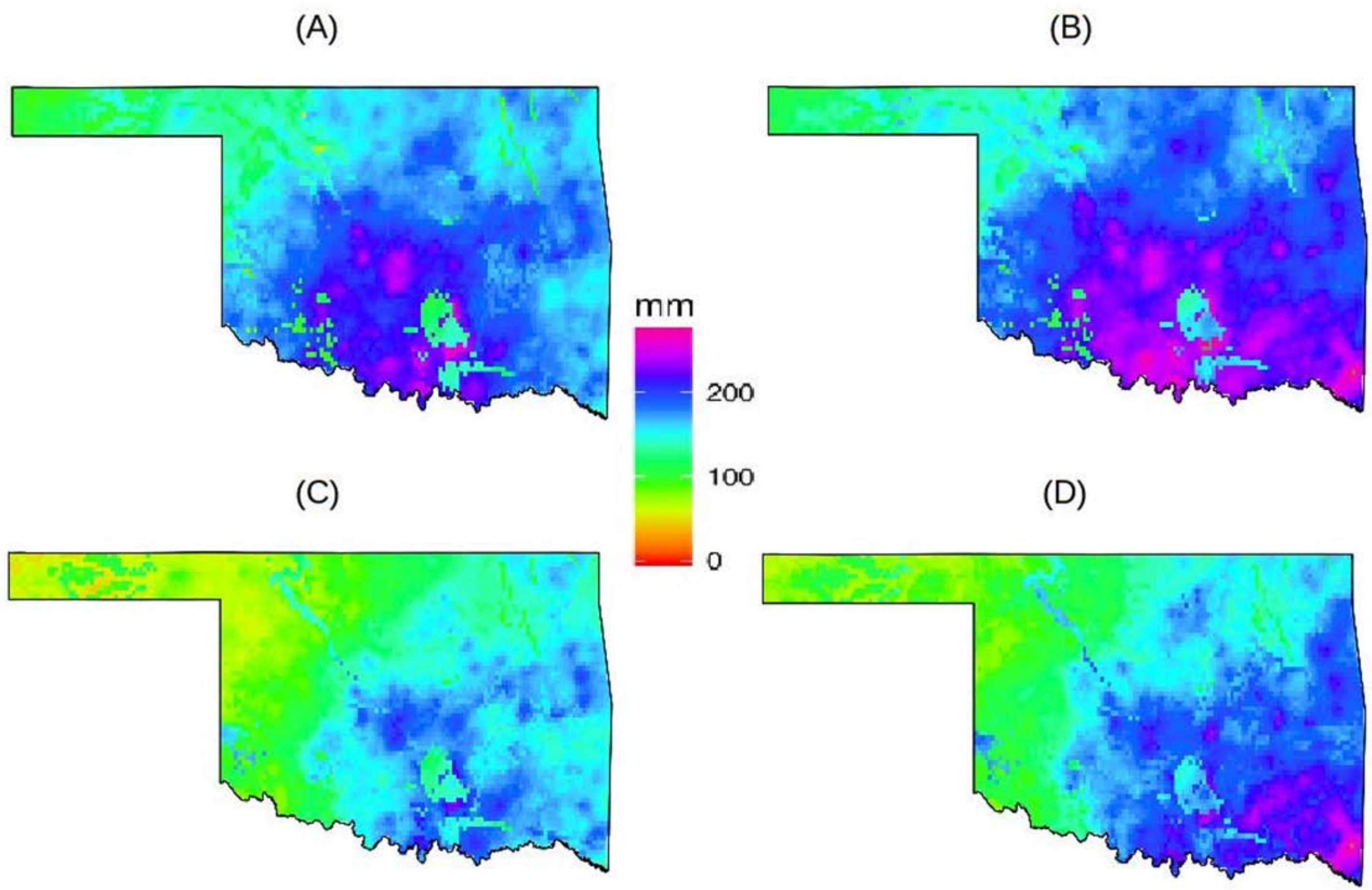

Figure 7: (A) Standard deviation in annual irrigation demand for corn with simulation starting 10 days before planting using STATSGO2 soil data at 50% initial soil moisture. Irrigation demand calculated by subtracting ET from rainfall. (B) Standard deviation in annual irrigation demand for corn with simulation starting 10 days after harvest using STATSGO2 soil data at 50% initial soil moisture. Irrigation demand calculated by subtracting ET from rainfall. (C) Standard deviation in annual irrigation demand for corn with simulation starting 10 days before planting using STATSGO2 at 50% initial soil moisture. Irrigation was applied at 6mm per application. Irrigation demand in calculated by subtracting ET from rainfall. (D) Standard deviation in annual irrigation demand for corn with simulation starting 10 days after harvest using STATSGO2 at 50% initial soil moisture. Irrigation was applied at 6mm per application Irrigation demand in calculated by subtracting ET from rainfall.

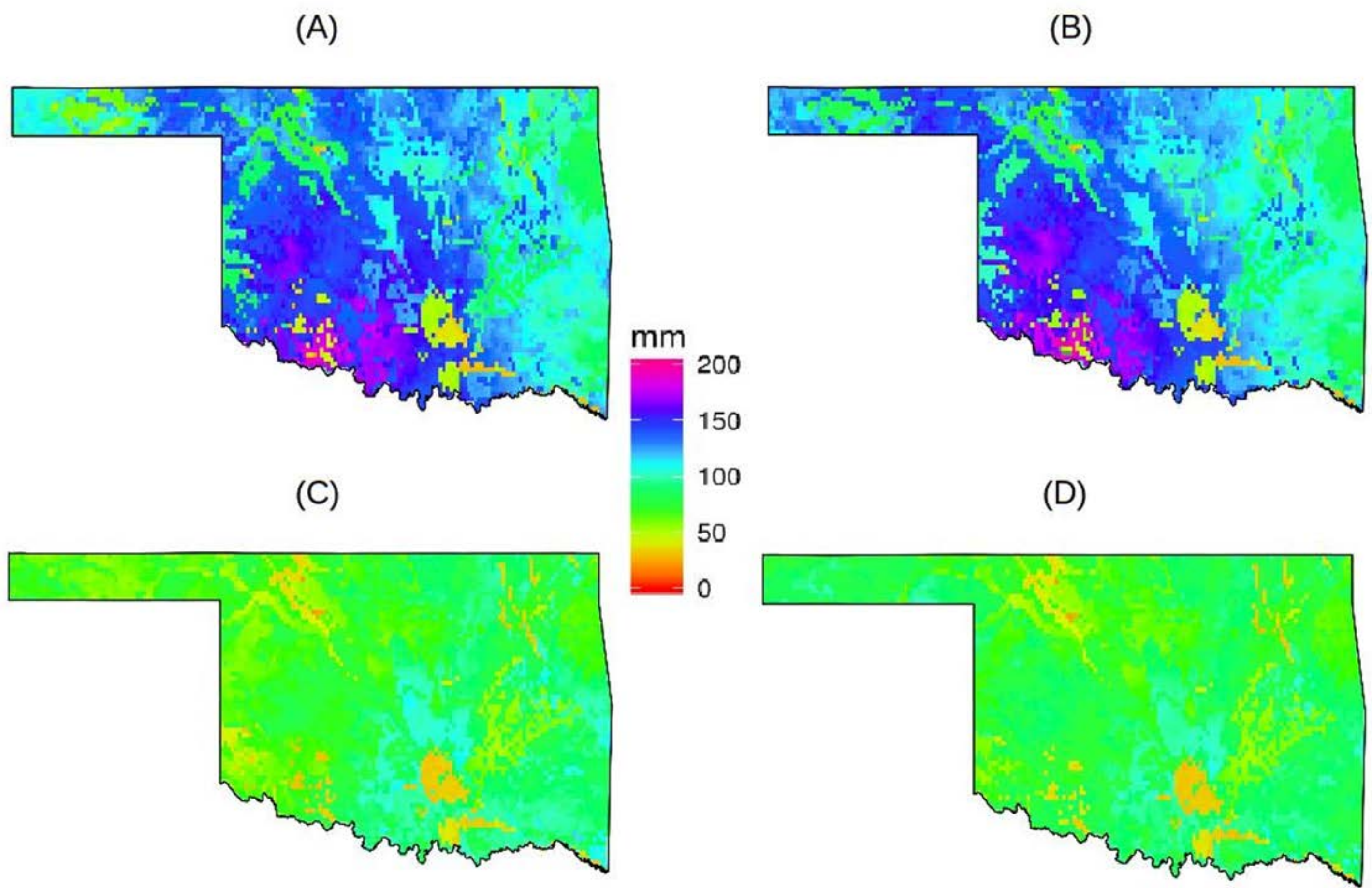

Figure 8: (A) Standard deviation in annual irrigation demand for cotton with simulation starting 10 days before planting using STATSGO2 soil data at 50% initial soil moisture. (B) Standard deviation in annual irrigation demand for cotton with simulation starting 10 days after harvest using STATSGO2 soil data at 50% initial soil moisture. (C) Standard deviation in annual irrigation demand for cotton with simulation starting 10 days before planting using STATSGO2 at 50% initial soil moisture. Irrigation demand in calculated using a fixed amount of 6 mm per applications. (D) Standard deviation in annual irrigation demand for cotton with simulation starting 10 days after harvest using STATSGO2 at 50% initial soil moisture. Irrigation demand in calculated using a fixed amount of 6 mm per applications.

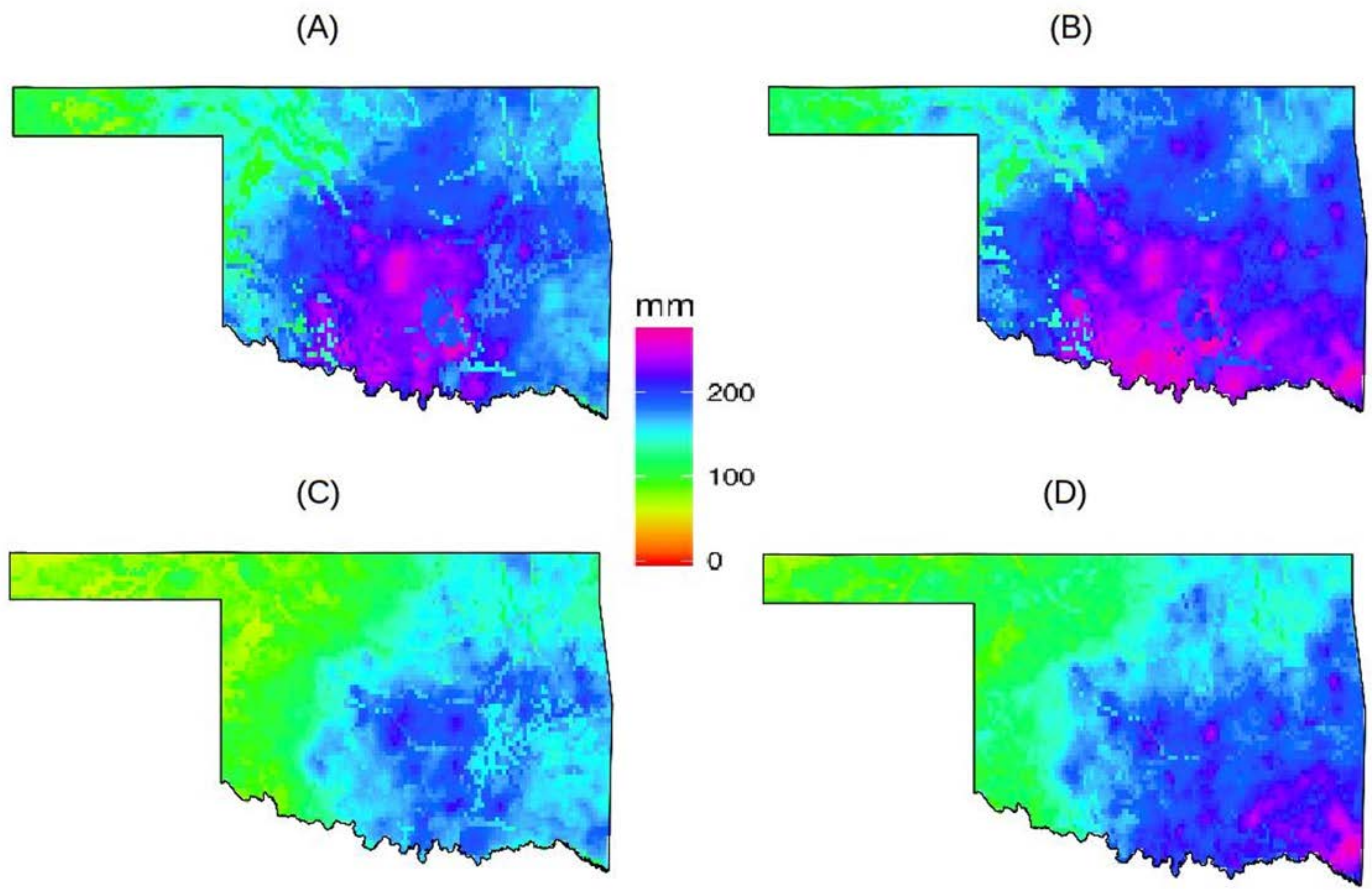

Figure 9: (A) Standard deviation in annual irrigation demand for cotton with simulation starting 10 days before planting using STATSGO2 soil data at 50% initial soil moisture. Irrigation demand calculated by subtracting ET from rainfall. (B) Standard deviation in annual irrigation demand for cotton with simulation starting 10 days after harvest using STATSGO2 soil data at 50% initial soil moisture. Irrigation demand calculated by subtracting ET from rainfall. (C) Standard deviation in annual irrigation demand for cotton with simulation starting 10 days before planting using STATSGO2 at 50% initial soil moisture. Irrigation was applied at 6mm per application. Irrigation demand in calculated by subtracting ET from rainfall. (D) Standard deviation in annual irrigation demand for cotton with simulation starting 10 days after harvest using STATSGO2 at 50% initial soil moisture. Irrigation was applied at 6mm per application Irrigation demand in calculated by subtracting ET from rainfall.

CHAPTER IV

GENERAL CONCLUSION

Crop models can be used to help determine the impact of climate variability (Rosenzweig et al., 1994; Lobell et al., 2008). Also, crop models can be used to access the risk involved in management decisions for prediction of irrigation water use. This could lead to a more effective way to manage more efficient to save money and resources. Chapter 2 shows the model was able to give a probabilistic forecast of wheat yield in Oklahoma, and reproduce the in-season variability of yield ranges across the season. The model was able to make a prediction as early as 5 to 15 weeks after planting at a 33% threshold, and 28 to 32 weeks after planting with a 10% threshold. The range of yield percentile is small enough to categorize into below average yielding, average yielding, and above average yielding. Initial conditions do play a role in model performance. Wheat yield forecasting can be a viable option for Oklahoma to aid in mitigating the effect of climate variability.

In Chapter 3, It was found DSSAT can be used to estimate irrigation demand in Oklahoma. Setting up the experiments in different ways can provide dramatically different results such as using fixed or fully irrigated simulations. Also calculating irrigation demand by ET-rain or letting DSSAT do the calculating. Using STATSGO2 soil data was the better soil data set to use because it shows a better distribution of soil depth than SoilGrids. Soil moisture seemed to work better when a spin-up period was used. Allowing DSSAT to calculate the irrigation demand using a fixed irrigation treatment with spin-up with STATSGO2 soil data at 50% soil moisture would probably give the best results if one was looking for the actual irrigation demand.

Chapters II and III both demonstrate how simulation modeling can be implemented to assist in solving issues where traditional field research cannot be applied. The limitations to the models are input data, initial conditions, and management practices. There is still a lot of room for improvement in the models discussed in this thesis, but it does provide a basis for future research.

REFERENCES

Rosenzweig, C., M. L. Parry, and others (1994), Potential impact of climate change on world food supply, *Nature*, *367*(6459), 133–138.

Lobell, D. B., M. B. Burke, C. Tebaldi, M. D. Mastrandrea, W. P. Falcon, and R. L. Naylor (2008), Prioritizing climate change adaptation needs for food security in 2030, *Science*, *319*(5863), 607–610.

VITA

Brandon Albin Vaverka

Candidate for the Degree of

Master of Science

Thesis: INITIAL EVALUATION OF SEASONAL YIELD AND IRRIGATION DEMAND FORECASTING FRAMEWORKS FOR OKLAHOMA

Major Field: Plant and Soil Science

Biographical:

Education:

Completed the requirements for the Master of Science in Plant and Soil Science at Oklahoma State University, Stillwater, Oklahoma in December, 2018.

Completed the requirements for the Bachelor of Science in Agronomy at Oklahoma Panhandle State University, Goodwell, OK in 2016.

Experience: Graduate Research Assistant at Oklahoma State University Department of Plant and Soil Sciences from August 2016 to June 2018. Soil Scientist internship at Natural Resources Conservation Service from June 2016 to August 2016. Tutor at Oklahoma Panhandle State University from January 2015 to May 2016. Soil Conservationist internship at Natural Resources Conservation Service from May 2015 to July 2015. Agronomy student worker at Hutchinson Community College from May 2014 to January 2015. Math tutor at Hutchinson Community College from August 2014 to January 2015. Student worker at Kansas State University Beef Cattle Research Center from April 2013 to August 2013 and April 2012 to August 2013.